# Organic Electrochemical Transistors as an Emerging Platform for Bio-Sensing Applications: A Review

Marios Sophocleous, *Member, IEEE*, Laura Contat-Rodrigo, Eduardo García-Breijo, and Julius Georgiou, *Senior Member, IEEE*

***Abstract*—Organic electrochemical transistors (OECTs) have been recognized as a major emerging technology in the area of flexible electronics in the last decade. Although they have yet to be incorporated in common electronic fabrication technologies, they have considerably advanced as an emerging platform for biosensing applications. The paper provides a comprehensive and critical review of the most important advances in the field of OECT-based biosensors. A brief description of the device physics is given with the most important equations and a comparison has been made with the conventional MOSFET devices and characteristic equations. The use of OECTs as an emerging biosensing platform has been explored and their application as biomolecule, enzyme, bacteria, viruses, cells, nucleotide detectors as well as electrophysiological and wearable sensors has been reported. Furthermore, trends have been extracted and described in the paper in terms of fabrication technologies, electrode materials and most importantly, the semiconducting polymer. Additionally, future perspectives on the development and fabrication technologies of these devices have been further explored.**

***Index Terms*—Biocompatibility, biosensors, high transconductance, Ion sensors, organic electrochemical transistors, OECTs.**
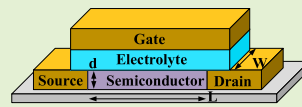
$$I_{DS} = \begin{cases} \mu C^* \frac{Wd}{L} \left[1 - \frac{V_{GS} - \frac{1}{2}V_{DS}}{V_{TH}} \right] V_{DS}, for\ V_{DS} > V_{GS} - V_{TH} \\ -\mu C^* \frac{Wd}{L} \frac{[V_{GS} - V_{TH}]^2}{2V_{TH}}, \quad for\ V_{DS} < V_{GS} - V_{TH} \end{cases}$$

$$g_m = \begin{cases} -\mu C^* \frac{Wd}{L} V_{DS}, \quad for\ V_{DS} > V_{GS} - V_{TH} \\ \mu C^* \frac{Wd}{L} [V_{GS} - V_{TH}], \quad for\ V_{DS} < V_{GS} - V_{TH} \end{cases}$$

I. INTRODUCTION

A TRANSISTOR is a device that has the ability to control, amplify, and modulate electrical signals. It consists of three main electrical terminals. Metal Oxide Semiconductor Field Effect Transistors (MOSFET) have source, drain and gate whilst Bipolar Junction Transistors (BJT) have emitter, collector and base as their electrical terminals [1]. Most common transistors available are silicon-based transistors, which can be found in almost every electronic device. Due to

Marios Sophocleous and Julius Georgiou are with the EMPHASIS Research Centre, Department of Electrical and Computer Engineering, University of Cyprus, 2109 Nicosia, Cyprus (e-mail: sophocleous.marios@ucy.ac.cy; julio@ucy.ac.cy).
Laura Contat-Rodrigo and Eduardo García-Breijo are with the Centro de Reconocimiento Molecular y Desarrollo Tecnológico, Group of Electronic Development and Printed Sensors (GEDPS), Unidad Mixta UPV-UV, Universitat Politècnica de Valéncia, 46022 Valencia, Spain (e-mail: lcontat@ter.up.es; egarciab@eln.upv.es).
Digital Object Identifier 10.1109/JSEN.2020.3033283

certain limitations of silicon electronic properties, other types of transistors are also available, such as germanium or gallium/arsenide and several indium compound-based transistors. In the last decade, another type of transistors has evolved featuring several advantages and disadvantages compared to the classical silicon-based transistors [2]. Organic transistors are a group of devices with the channel between source and drain being made up of organic semiconductors [3]. They are similar to Thin Film Transistors (TFT) as they do not have a substrate contact, commonly found in MOSFETs.

Organic transistors are usually separated into two main categories: Organic Field-Effect Transistors (OFETs) [4] and Organic Electrochemical Transistors (OECTs) [5]. OFETs are very similar to the classic field-effect transistors with the difference that the semiconducting material is organic [6]. In OECTs on the other hand, the organic semiconducting channel is in contact with an electrolyte in which the gate electrode is immersed [7]. The operation of an OECT is based on the injection of ions into the organic film through the electrolyte [8]. This changes the doping state of the film and therefore, its conductivity. Voltages, applied at the three terminals of the device, control the doping rate and state of the device, hence controlling its behavior in a similar manner to traditional transistors [9]. Although these devices do not have complementary structure as in metal-oxide semiconductors (CMOS),

and compatibility and reliability of the classical transistors is much higher at this time, OECTs feature some significant advantages [2]. The gate-channel capacitances of these devices can reach up to 9 mF •cm^{-2}, which is more than three orders of magnitude greater than what can be achieved with state-of-the-art high-κ dielectrics [9]. This feature is a result of the electrolyte double layers and the ability of the ions to penetrate into the organic semiconductor [10]. Subsequently, due to these high capacitances, OECTs can operate at very low voltages ($\sim$0.5 V) and have impressive transconductances of more than 800 Sm^{-1} (in some extreme cases, up to 7000 Sm^{-1}), much higher than any classical transistor technology. Furthermore, these organic semiconducting materials are flexible (with Young moduli of $\sim$100 MPa), biocompatible and can be solution processed (low-cost fabrication ($\sim$€5)) [11]. These unique properties of OECTs have led researchers to use them in a very wide variety of applications, like digital logic, low power electronics, flexible electronics, neuromorphic engineering and sensing [12]. As the state-of-the-art in the field of OECTs is progressing, more research is directed towards sensing applications, in particular to biosensing, with some very impressive detection limits (fM range) due to the very high transconductance achieved [13]. Additionally, due to the very low voltages used, living cells and other living organisms can most of the times be detected without affecting them [14]. Moreover, the biocompatibility of the devices together with their flexibility are ideal for implanted devices in the human body [15].
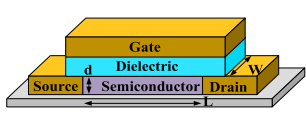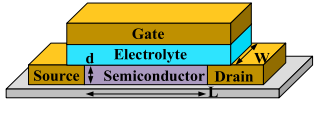
In this review, the operating principles of OECTs based on the Bernard model will be compared with classical MOSFET and a comprehensive and critical review of the advances in the field of biomolecule, enzyme, bacteria, viruses, cells, nucleotide detection as well as electrophysiological and wearable sensors, using OECTs will be explored. Trends in the semiconducting materials and fabrication technologies will be further explained with predictions for future directions on OECTs, as an emerging platform for biosensing applications.

II. DEVICE PHYSICS

Semiconducting materials used in OECTs can, like in MOSFETs, be either n-type conducting electrons or p-type conducting holes, or even amphipolar [16]. However, most organic semiconductors are p-type, due to their better robustness and stability. The most commonly used organic semiconductor is poly(3,4-ethylenedioxythiophene) polystyrene sulfonate (PEDOT:PSS), which is a p-type semiconductor. The reason is its low cost (<€1/gram), compatibility with the majority of fabrication technologies, high transconductance, better reliability, biocompatibility and easier manufacture than other organic semiconductors [17], [18].

In most cases of using OECTs, the source is grounded and a bias voltage is applied to the drain electrode driving a current, I_{DS}. If no voltage (V_{GS}) is applied to the gate electrode, then the current will depend on the intrinsic properties of the organic semiconductor used in the channel [9]. However, when a voltage is applied at the gate electrode, then ions from the electrolyte cause de-doping of the organic semiconductor and the conductivity of the semiconductor changes, changing I_{DS}.

TABLE I
A COMPARISON OF OECTS AND MOSFET STRUCTURES & CHARACTERISTICS

Structure (p-type)

Drain-Source Current*

MOSFET (Linear Range)

$$I_{SD} = \mu C_{ox} \frac{W}{L} \left[(V_{SG} - |V_{TH}|)V_{SD} - \frac{V_{SD}^2}{2} \right] (1 + \lambda V_{SD}) \quad (1)$$

OECT (Linear & Saturation Range)

$$I_{DS} = \begin{cases} \mu C^* \dfrac{Wd}{L} \left[1 - \dfrac{V_{GS} - \frac{1}{2}V_{DS}}{V_{TH}} \right] V_{DS}, for\ V_{DS} > V_{GS} - V_{TH} \\ -\mu C^* \dfrac{Wd}{L} \dfrac{[V_{GS} - V_{TH}]^2}{2V_{TH}}, \qquad for\ V_{DS} < V_{GS} - V_{TH} \end{cases} \quad (2)$$

Transconductance*

MOSFET (Linear Range)

$$g_m = \mu C_{ox} \frac{W}{L} (V_{SG} - V_{TH}) \quad (3)$$

OECT (Linear & Saturation Range)

$$g_m = \begin{cases} -\mu C^* \dfrac{Wd}{L} V_{DS}, \qquad\quad for\ V_{DS} > V_{GS} - V_{TH} \\ \mu C^* \dfrac{Wd}{L} [V_{GS} - V_{TH}], \qquad for\ V_{DS} < V_{GS} - V_{TH} \end{cases} \quad (4)$$

W, L and d are channel width, length and thickness (m), respectively; μ is the charge-carrier mobility (m^2 V^{-1} s^{-1}); C (C m^{-3}) represents the $\mu q \rho_0$ constant where q is charge (C) and ρ_0 is the initial hole density (m^{-3}); V_{DS}, V_{GS} and V_{TH} are the drain, gate and threshold voltages, respectively [9], [11].

In most cases, the diffusion of ions in the organic semiconductor, or gate current, features a purely capacitive behavior since the source and drain electrodes block the ions and do not allow direct faradaic charge transfer. However, that depends on the type of gate material used [3], [14]. Hence, this effect is only observed in the transient behavior of the transistor whilst it vanishes in the steady state. The most common model used to describe the behavior of OECTs is the Bernard model [9] and has significant similarities with the classical MOSFET model. The equations given are adjusted for the most common p-type semiconductor. The general structure of OECTs is given in Table I with a comparison to conventional MOSFETs.

A comparison of current-voltage characteristics between p-type MOSFETs and PEDOT:PSS-based OECTs is given in Figure 1 below visually showing the significant similarities and differences between the two device types [11], [19].

The transconductance of the transistor (g_m) is defined as the ratio of the change in current I_{DS} at the output terminal to the change in the voltage V_{GS} at the input terminal of an active device [8].

In sensing applications, transconductance is of high importance since this property is usually the one proportional to the parameter of interest. Therefore, a small change in the gate voltage gives a large change in the channel current, which allows for high resolutions and lower limits of detection [20].
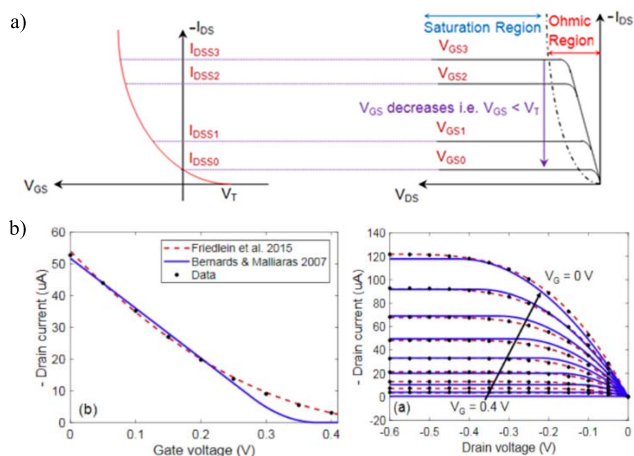
Fig. 1. a) I-V characteristic curves of p-type MOSFET [19], b) I-V characteristic curves of PEDOT:PSS-based OECTs [11].
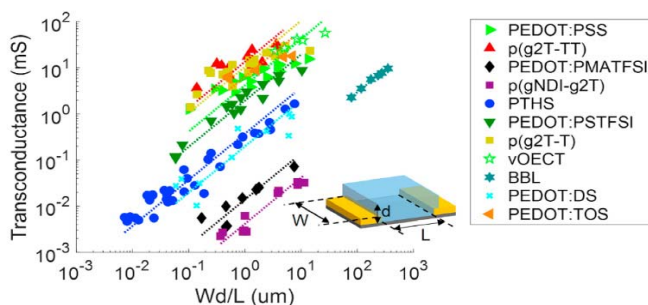

Fig. 2. Transconductance ranges for different organic semiconducting materials. The dotted lines are best fits of $g_m = \alpha Wd/L$, where α is a proportionality constant that is different for each data series [11].
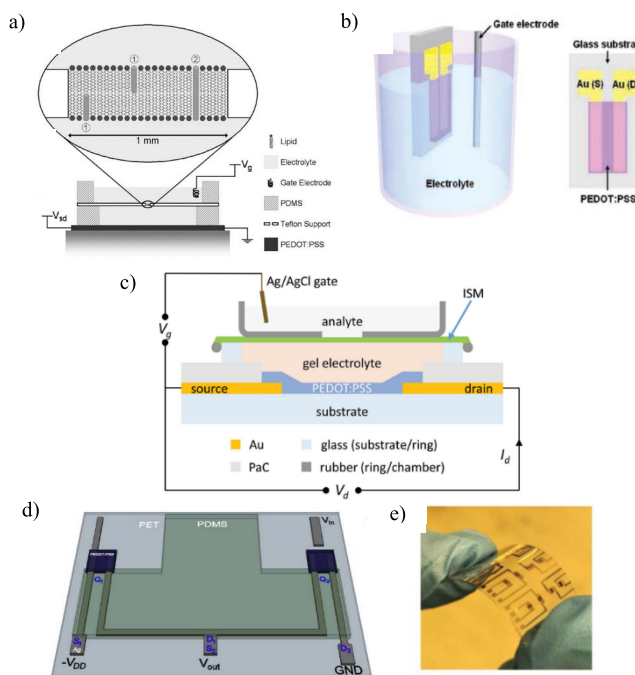

Fig. 3. a) Schematic of PEDOT:PSS electrochemical transistor gated through a bilayer lipid membrane (reproduced from [22] with permission from AIP Publishing, Copyright © 2006), b) Schematic of a PEDOT:PSS-based OECT (reproduced from [23] with permission from American Chemical Society, Copyright © 2010), c) Cross section schematic and wiring of the IS-OECT (reproduced from [24] with permission from John Wiley and Sons, Copyright © 2014), d) 3D rendering of the inverter design (reproduced from [26] with permission from Elsevier, Copyright © 2019), e) Photograph of PEDOT:PSS/[EMIM][TCM] OECTs (reproduced from [27] with permission from John Wiley and Sons, Copyright © 2018).

Several organic semiconducting materials have been used by researchers covering a wide range of transconductances (Figure 2).

The next sections provide a critical review of the reported OECTs used for biosensing applications [11].

III. ION SENSORS

Ion concentrations in biological media play a major role in the health of every organism. Hence, the ability to monitor those concentrations accurately, fast and at low cost has generated the need for the development of ion sensors for biological media. However, classical ion sensors have low sensitivities, obeying the Nernstian response of 59.2 mV/$\log_{10}[C_{Ion}]$ for monovalent ions at 25°C. Therefore, conducting polymers and OECTs have been implemented to develop ion sensors with higher sensitivities, much higher ion-to-electron conversion and better signal-to-noise ratios compared to other Solid-State Ion-Selective-Electrodes. Additionally, their ability to convert low ionic currents to high electronic currents, make them ideal for ion sensing applications in biological media. Nevertheless, some OECT-based ion sensors have shown sensitivities close to the Nernstian response, which also can be achieved with other available sensors. However, when the high transconductance of the OECTs was properly utilized, they have shown sensitivities of up to 600 mV/ $\log_{10}[C_{Ion}]$ [21]. The reported

Limits of Detection (LODs) have a long way to go when compared to sensors involving nanotechnologies and Carbon Nano Tubes (CNT). The reported LODs for OECT-based ion sensors are in the micromolar range whilst nanotechnology sensors can reach down to the picomolar range.

A. Cation Sensing

In 2006, Bernard *et al.* [22] reported the use of a bilayer lipid membrane as a means to control the gating of an OECT (Figure 3a). It was shown that it is possible to distinguish between solutions of monovalent (K^+) and divalent (Ca^{2+}) cations using the valence-dependent permeability of gramicidin ion-channels in a PEDOT:PSS-based OECT. This property was further investigated by Lin *et al.* [23] where they used a very simple OECT device with gold (Au) drain and source electrodes and Cr/Au, Ag/AgCl and Pt gate electrodes (Figure 3b). They systematically studied the ion-sensitive behavior of OECTs based on PEDOT:PSS in aqueous solutions with different cations, including H^+, K^+, Na^+, Ca^{2+}, and Al^{3+}. The effective gate voltage was found to be proportional to the concentration of cations in the electrolyte featuring an almost Nernstian response. Additionally, it was observed that the gate electrode plays an important role on the device performance, giving a better understanding of the physical and chemical OECTs mechanism. The de-doping process was described

using the following reaction [23]:

$$n(PEDOT^+ : PSS^-) + M^{n+}$$
$$+ ne^- \rightleftharpoons nPEDOT^0 + M^{n+} : nPSS^- \quad (5)$$
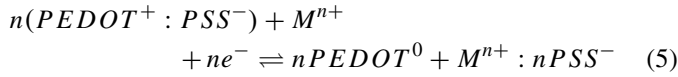
As the concentration of cations in the electrolyte increases, the transfer curves of the OECTs shift to lower gate voltage horizontally. A Nernstian response was observed when a Ag/AgCl gate electrode was used. In the cases where Pt and Au were used as gate electrodes, different sensitivities have been recorded, higher than the Nernstian response.

Other researchers have later focused on specific ions such as K^+. In 2014, Sessolo et al. [24] brought the conducting polymer in direct contact with a reference gel electrolyte with an ion-selective membrane hence, utilizing the high transconductance of the devices (Figure3c). The authors have demonstrated that OECTs are strong candidates for solid-state ion sensors featuring a sensitivity of approximately 50 μA/decade of potassium concentration in the range of 10^{-4} to 10^{-1} M and showing significant selectivity when compared to similar cations such as sodium. In 2018, Ghittorelli et al. [25] demonstrated for the first time that the sensitivity limitations of classical transistor-based approaches can be overcome with the use of OECTs. They have successfully shown ion sensitivity of 414 mV/decade of potassium concentration and 516 mV/decade of sodium concentration, which are by an order of magnitude higher than any other reported electrochemical ion sensor.

Utilizing the rise of 3D printing technologies, Majak et al. [26] demonstrated a 3D printed inverter logic gate sensor based on an OECT with PEDOT:PSS as the ion sensitive channel material (Figure3d). The devices were tested in various electrolytes and it was demonstrated that the inverter logic gate can be used reliably as a cation type and concentration sensor. For the described devices a limit of detection of 1mM for NaCl, CaCl$_2$ and KCl electrolytes was found. These sensors feature a very high sensitivity of 650 mV/decade and 200 mV/decade in the range of the 1–100 mM and 100–1000 mM for Na^+ ions, respectively. It was concluded that the type of cation being detected could be identified based on the switching voltage shift of these devices. Wu et al. [27] on the other hand, have shown an OECT-based sodium Na^+ sensor with PEDOT:PSS doped with ionic liquid 1-ethyl-3-methylimidazolium tricyanomethanide ([EMIM][TCM]) as the active channel (Figure3e) that exhibits a record high transconductance of $\approx$7100 Sm^{-1} and fast transient response of 3.9 ms. The strong affinity of the ionic liquid with PEDOT:PSS also translates to a relatively high biasing (VG $\sim$ 0.8 V) required for switching the OECT to off state.

B. pH Sensing

Other than cation sensing, OECTs were also used as pH sensors with sensitivities higher than Nernstian however, some of those devices did not cover the whole pH range. In 2017, Scheiblin et al. [28] reported a pH sensor without a reference electrode based on an screen-printed OECT that was integrated in a differential bridge (Figure 4a). This circuitry allows
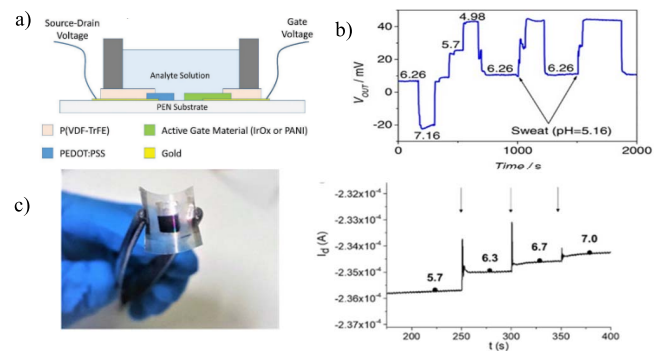

Fig. 4.   a) Cross-section schematic of the pH sensor (reproduced from [28] with permission from John Wiley and Sons, Copyright © 2016), b) Output voltage of a printed bridge upon addition of ideal buffer solution at known pH and human sweat sample in the sensing well, the reference well was filled by a reference buffer solution at pH = 6.26 (reproduced from [28] with permission from John Wiley and Sons, Copyright © 2016), c) (left) Flexible OECT pH sensor, (right) I_d versus time curve recorded in artificial sweat with base equimolar additions (Vg= −0.1V; Vd= −0.2V) (reproduced from [29] with permission from the American Chemical Society, Copyright © 2018).

biochemical sensing without the use of a reference electrode. The OECT was based on electrodeposited iridium oxide gate electrodes that enable pH measurements with increased sensitivity of 9.5 μA/pH within the pH range of 5-7.3 in human sweat (Figure 4b).

Mariani et al. [29] reported highly sensitive pH sensing (93 mV/pH) by successive sampling in aqueous electrolytes. Two PEDOT composites, doped with pH dyes (Bromothymol Blue and Methyl Orange), have been optimally synthesized as pH-sensitive conducting polymers with the ability to convert pH into electrical signal. PEDOT:BTB composite demonstrated the best performance and was used as a gate electrode in the development of an OECT-based pH sensor operating in a two-fold transduction mode with super-Nernstian sensitivity. The offset gate voltage of the sensor shifts by $(1.1\pm0.3)\times10^2$ mV/pH when the pH of a medium is dynamically changed. Moreover, further work has been done using the optimized configuration on PET whilst the performance of PET-based OECT was evaluated in artificial sweat within a medically relevant pH range (Figure 4c).

IV. BIOMOLECULE/ENZYME SENSORS

OECTs can operate stably in aqueous environments, which is essential for biological sensing. OECTs are most of the times biocompatible and operate at low voltages. Therefore, OECTs have been applied in organic bioelectronics to monitor the concentration of various types of biological analytes. Most common approach to biomolecule detection is based on enzymes and usually oxidazes that have hydrogen peroxide as a byproduct that reacts with the electrode and generates current. The current is proportional to the concentration of the measurant however; there are several issues with noise and subsequently the LOD. OECT-based sensors for biomolecules and/or enzymes have achieved sensitivities up to several μA/$\log_{10}$[C] and with LODs down to the nanomolar range. Nevertheless, more work is required for these devices to reach the nanotechnologies levels but these sensors are good enough

for use in biological samples since they fall within the required ranges.

A. Glucose Sensing

OECTs applied as glucose sensors have attracted particular attention due to their high sensitivity, and their suitability for non-invasive detection of glucose in saliva with extremely low glucose concentrations featuring excellent potential in replacing traditional testing methods.

Macaya et al. were one of the first groups that reported the application of OECTs in glucose sensors [30] after the work from Bartlett et al. [31] and Zhu et al. [32]. They initially developed PEDOT:PSS-based OECTs with platinum (Pt) gate electrode for glucose detection. Operation of these devices is based on the enzymatic reaction between glucose and glucose oxidase (GOx), and further oxidation of the hydrogen peroxide (H_2O_2) generated from the glucose oxidation, by the Pt electrode (Figure 5a). The additional gate current caused by the oxidation of H_2O_2 at the Pt electrode de-dopes the PEDOT:PSS channel, leading to a decrease of the drain current that is proportional to the glucose concentration. They demonstrated that the enzyme GOx does not need to be immobilized but can be simply added in the electrolyte solution, without any surface modification of the gate and the transistor channel. Not immobilizing the enzyme greatly simplifies device fabrication and decreases detection time significantly, since glucose does not have to diffuse to react with the enzyme. They showed that these OECTs can be successfully used to detect glucose in the micromolar range, well within the range of glucose levels in saliva [10]. The sensitivity and detection range of these sensors can be tuned by adjusting the magnitude of the gate bias. Increasing the gate bias leads to a smaller response due to a competition between glucose-induced de-doping and de-doping by cations in the electrolyte. The latter is enhanced at higher values of the gate bias, decreasing the device sensitivity.

However, the use of Pt electrodes complicates the device fabrication and increases cost, being highly desirable to replace it with a low-cost material. Kanakamedala et al. [33] developed an enzymatic sensor for glucose detection entirely made out of polymer. They fabricated an all-PEDOT:PSS OECT in a one step process using xurography, an inexpensive and rapid technique, that allows the transistor to be patterned on a flexible substrate. The sensing mechanism was also based on the enzymatic oxidation of glucose, producing H_2O_2 that is further oxidized by PEDOT:PSS, without any external electron mediator. Upon the addition of glucose, the drain current decreases due to the reduction of the PEDOT:PSS channel by H_2O_2 (Figure 5b). De-doping of the polymer channel depends on the glucose content. By optimization of the gate and channel dimensions, the sensor achieved glucose detection in the 1-200 μM concentration range, which is relevant for glucose detection in saliva, with a sensitivity of 0.01 Normalized Response (NR)/μM.

The sensing method based on the measurement of H_2O_2 suffers from higher oxidation potential requirement and difficulty in analyzing higher glucose concentrations. To overcome this issue, the group of Malliaras designed a glucose sensor based
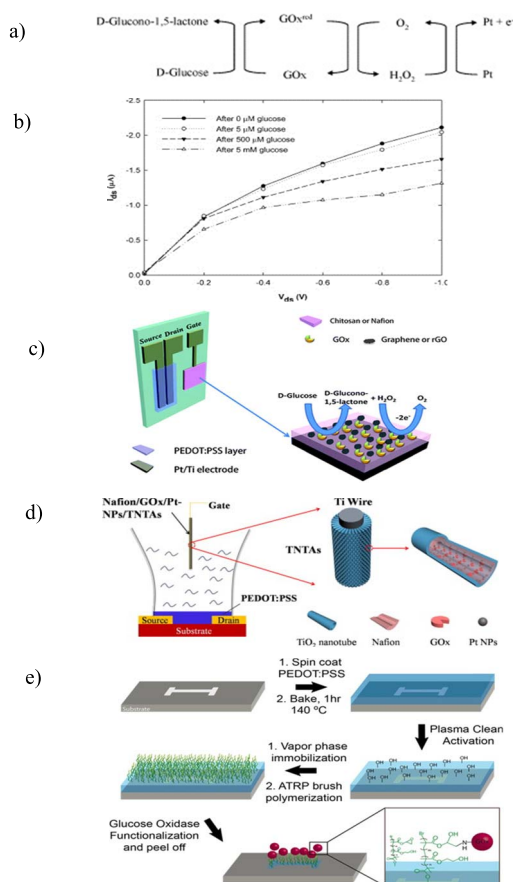

Fig. 5. a) Reaction cycle for glucose detection with the enzyme GOx and Pt gate electrode (reproduced from [30] with permission from Elsevier, Copyright © 2007), b) Response of drain current (I_{DS}) as a function of drain voltage (V_{DS}) in the presence of different glucose concentrations (reproduced from [33] with permission from Elsevier, Copyright © 2011), c) Schematic diagram of an OECT-based glucose sensor modified with GOx, chitosan (Nafion) and graphene (rGO) flakes (reproduced from [37] with permission from Elsevier, Copyright © 2015), d) Schematic diagram of the OECT-based glucose sensor with Nafion/GOx/Pt-NPs/TNTAs gate electrode, Au/Cr source and drain electrodes, and PEDOT:PSS active channel on glass substrate (reproduced from [39] with permission from the Royal Society of Chemistry, Copyright © 2013), e) PGMA:PHEMA mixed polymer brush fabrication on the device and functionalization with GOx (reproduced from [29] with permission from John Wiley and Sons, Copyright © 2014).

on an all-PEDOT:PSS OECT and ferrocene mediator [34]. The charge transfer reaction that takes place at the gate electrode decreases the potential drop at the gate/electrolyte interface. The potential drop at the electrolyte/channel interface increases as the gate electrode is held at a fixed bias with respect to the channel. This results in more effective gating of the transistor channel and the drain current decreases, in a way that depends on glucose concentration. The device can detect glucose down to the micromolar range and can be fabricated using a one-layer patterning process. Based on this enzymatic sensor, they later fabricated a new type of glucose sensor by integration of an all PEDOT:PPS-OECT with a Room Temperature Ionic Liquid (RTIL) as electrolyte, thus solving issues related to long term stability of the OECTs for use in biosensing [35]. RTILs are molten salts that are entirely

composed of ions and are at liquid state at ambient temperature. In electrochemistry, RTILs can be used as alternatives to aqueous electrolytes like PBS. In this device, the RTIL is used as an immobilization medium for GOx and the ferrocene (Fc) mediator. Upon addition of the aqueous solution containing the analyte, the enzyme and the mediator dissolved in the RTIL. This sensor can detect glucose in the 10^{-7} to 10^{-2} M concentration range.

In real applications for *in vivo* monitoring of glucose, it is more convenient to immobilize GOx either on the gate electrode or the active channel, in order to prevent enzyme leakage and signal decrease over time. In terms of **gate functionalization**, Tang *et al.* [36] first presented novel highly sensitive OECT-based glucose sensors by modifying Pt gate electrodes with nanomaterials (multi-wall carbon nanotubes (MWCNTs) or Pt nanoparticles (Pt-NPs)), chitosan (CHIT) and GOx. The devices show considerable improvement of the sensitivity and the detection limit, which was extended down to 5 nM when the gate electrode was modified with Pt-NPs. The improvement of the sensor performance is attributed to the excellent electrocatalytic properties of nanomaterials and the more efficient enzyme immobilization on the gate electrode, due to their large surface area and good biocompatibility in keeping enzymatic bioactivity. However, these devices exhibit poor linearity of the response to glucose, which may be a drawback for practical applications. To overcome this, the group of Yan [37] reported OECT-based glucose sensors with increased sensitivity and selectivity by modifying the Pt gate electrodes with graphene-based materials (graphene or reduced graphene oxide (rGO)), biocompatible polymers (CHIT or Nafion) and GOx (Figure 5c). Graphene and rGO extend the detection limit and improve the sensitivity of the devices, since they enhance the charge transfer and the surface to volume ratio of the gate electrode. CHIT and Nafion help immobilization of GOx on the gate electrode and enhance the selectivity of the devices. The optimized device with CHIT and graphene exhibits logarithmic response to glucose in a broad concentration range from 10 nM to 1 μM, with detection limit down to 10 nM. The interfering effect caused by uric acid (UA) and ascorbic acid (AA) was found to be negligible for practical applications.

Based on these devices, Liao *et al.* [38] fabricated glucose sensors based on OECTs with Pt gate electrodes modified with Nafion-graphene composite, followed by a thin layer of polyaniline (PANI) conducting polymer. GOx was immobilized on the PANI surface via effective chemical covalent bonding. Graphene flakes improve the electrocatalytic activity and the conductivity of the gate electrode. The PANI film is in the protonated emeraldine salt form, which can strongly repel the positively charged molecules (like dopamine) in PBS solution by electrostatic forces. On the other hand, Nafion is negatively charged in PBS solution and can effectively hinder the diffusion of anionic electroactive species (like AA and UA) through it by electrostatic interactions. Therefore, the PANI/Nafion-graphene bilayer film can block the diffusion of both positively and negatively charged molecules to the Pt gate electrode, improving the selectivity of the device. These biosensors show a detection limit of 30×10^{-9} M and excellent selectivity for practical applications.

These OECT-based glucose sensors are equipped with Pt-gate electrodes, which is an expensive metal. Liao *et al.* [39] reported a high-performance low-cost ($<\euro 10$) OECT-based glucose sensor using TiO_2 nanotube arrays (TNTAs) as gate electrode. TNTAs have good biocompatibility, large surface area, excellent electron-transfer behavior and large number of active sites for chemical reactions, making them ideal substrate for biosensing. They fabricated highly sensitive and selective OECTs by modifying TNTAs electrodes with Pt nanoparticles (Pt-NPs), GO_x and Nafion (Figure 5d). Pt nanoparticles (Pt-NPs) significantly improve the sensitivity, owing to their excellent conductivity and electrocatalytic properties. The device shows a logarithmic response to glucose concentration over the range 100 nM – 5 mM, with sensitivity of 0.009 Normalized Current Response (NCR)/decade and detection limit as low as 100 nM. On the other hand, the biocompatible polymer Nafion considerably increases the selectivity of the sensor towards negatively charged interferences such as AA and UA. The device exhibits good stability and reproducibility.

In terms of **channel functionalization**, GO_x can also be immobilized in the transistor channel. Welch *et al.* [40] developed a glucose sensor by incorporation of polymer brushes to an OECT. Polymer brushes are biocompatible and have the ability to covalently bond enzymes and other biomolecules to different surfaces. A mixed polymer brush of poly(glycidyl methacrylate) (PGMA) and poly(2-hydroxyethyl methacrylate) (PHEMA) was polymerized from the surface of the PEDOT:PSS channel and functionalized with GO_x (Figure 5e). The devices exhibit a strong response to glucose in the 10 μM-100 mM concentration range, which covers physiological and pathological glucose levels in human blood and saliva. The devices also show remarkable stability over a time-period of 100 days.

B. Neurotransmitter Sensing

Dopamine (DA) is a neurotransmitter that plays an important role in the functions of central nervous, renal, and cardiovascular systems. The imbalance or dysfunction of dopamine result in various serious diseases. Tang *et al.* [41] assessed the use of PEDOT:PSS-based OECTs as DA sensors. The sensitivity of the OECT sensor depends on the gate electrode and operation voltage. Different types of gate electrodes were compared, including graphite (G), Au and Pt electrodes. Additionally, G and Pt electrodes were modified with multi-walled carbon nanotubes (MWCNTs)-chitosan (CHIT) hybrid. The sensing mechanism is based on the electrochemical detection of DA at the gate electrode (Figure 6). The highest sensitivity was obtained for the device with Pt gate electrode working at a gate voltage of 0.6 V. This optimized OECT can detect DA with a detection limit lower than 5 nM, being potentially useful for the determination of DA in clinical applications.

Epinephrine is an excitatory neurotransmitter, which plays an important role in cardiac, muscular and liver functions. The group of Yan [42] reported highly sensitive epinephrine sensors using PEDOT:PSS-based OECTs fabricated by a facile, low cost solution process. The device performance was
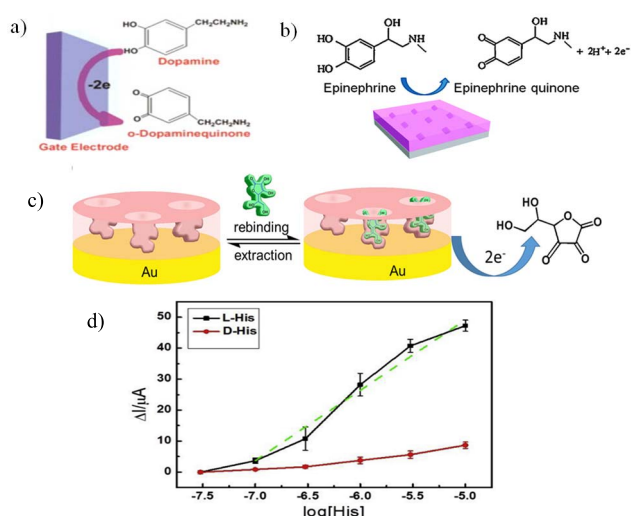
Fig. 6. a) Electro-oxidation of dopamine at the surface of the gate electrode (reproduced from [41] with permission from Elsevier, Copyright © 2011), b) Electro-oxidation of epinephrine at the surface of the gate electrode (reproduced from [42] with permission from the Royal Society of Chemistry, Copyright © 2013), c) Schematic of the removal and rebinding of AA on the MIP film surface, and the oxidation of AA on the modified Au gate electrode (reproduced from [49] with permission from Elsevier, Copyright © 2018), d) Channel current change ($_{\Delta ID}$) of OECT devices modified with L-His MIP films vs. D/L-His concentration in PBS (pH 7.4) at fixed VG = 0.6V and VD = 0.02V (reproduced from [51] with permission from Elsevier, Copyright © 2018).

optimized by immobilizing biocompatible polymer Nafion and carbon-based nanomaterials (single-walled carbon nanotubes (SWCNTs), graphene (Gr) and graphene oxide (GO)) on the Pt gate electrode. The working mechanism is based on the direct electro-oxidation of epinephrine at the gate electrode (Figure 6b). Consequently, the channel current decreases with the increasing concentration of epinephrine. The negatively charged Nafion can enhance the sensitivity of the device by attracting positively charged epinephrine molecules in neutral PBS solution by electrostatic interactions, to increase the concentration of epinephrine near the gate electrode. Carbon-based nanomaterials can further improve the sensitivity and decrease the detection limit of the biosensor, due to the enhanced electrocatalytic activity of the gate electrode. The device with Nafion/SWCNTs modified Pt gate displays a detection limit down to 0.1 nM, which is sensitive enough for medical applications. Moreover, Nafion can also improve the selectivity of the devices to the negatively charged interferences, AA and UA, by effectively blocking their diffusion to the Pt gate electrode by electrostatic interactions.

Later, Saraf *et al.* [43] reported a novel PEDOT:PSS-based OECT with aptamers modified Au gate electrode to detect epinephrine. Aptamers are short DNA and RNA chains which selectively bind to a target molecule with high affinity, that are extensively used as biorecognition molecules. The addition of epinephrine results in a significant decrease of the channel current according to a sensing mechanism similar to that previously described by Mak *et al.* [42]. The high binding affinity of the aptamers towards epinephrine and its electro-oxidation at the Au gate electrode allow this biosensor to show

a detection limit as low as 90 pM. Moreover, the device shows an instant drop in current upon addition of epinephrine as opposed to other interfering molecules (DOPAC, tryptophan, tyrosine, glycine, cysteine, DA, AA), that indicates highly selective nature of the sensor.

Kergoat *et al.* [44] reported the use of OECTs for the enzymatic detection of two of the main neurotransmitters in the human body: **glutamate and acetylcoline**. By incorporation of Pt nanoparticles (Pt-NPs) into PEDOT:PSS, they fabricated selective and sensitive OECTs for the detection of neurotransmitters, with all three electrodes and the channel composed of such PEDOT:PSS/Pt-NPs composite. Enzymes were immobilized at the surface of the gate electrode, by using an immobilization strategy based on enzyme crosslinkers. Glutamate is directly oxidized by glutamate oxidase (GluOx), producing H_2O_2.

In contrast, since acetylcholine does not have a specific oxidoreductase, a combination of two enzymes is needed. The first enzyme, acetylcolinesterase (AchE), transforms the acetylcholine into choline, that is then oxidized by cholesterol oxidase (ChOx). The amount of H_2O_2 is directly proportional to that of the neurotransmitter. These biosensors exhibit a sensitivity of 4.3 mol/l.cm^2 and 4.1 mol/l.cm^2 for glutamate and acetylcoline, respectively. Detection limits of 5 μM were obtained for both neurotransmitters. Therefore, these devices can detect glutamate down to concentrations found in the body fluids. In contrast, although they can also detect acetylcoline at low concentrations, these are not low enough to enable monitoring of this neurotransmitter in extracellular fluids.

C. Liposomes Sensing

Liposomes are good candidates as nanocarriers for reliable and efficient drug delivery due to, among others, their biocompatibility, the ability to entrap both hydrophilic drugs in the inner area and hydrophobic drugs into the membrane, and their selectivity to the target. Tarabella *et al.* [45] reported the use of PEDOT:PSS-based OECTs integrated in microfluidics for sensing liposomes (lecithin, L) and liposome-based nanoparticles (lecithin-chitosan, LC) in electrolyte solutions. They showed that the OECTs are efficient, reliable and sensitive devices for sensing these analytes. The devices can detect L liposomes on a dynamic range down to 10^{-4} mg/ml, and LC nanoparticles on a wider range, starting from 10^{-5} mg/ml, well within the range of interest for nanomedicine and drug delivery applications. The OECTs detection sensitivity is extended by real-time monitoring, with lowest LC nanoparticles detection limit of 10^{-7} mg/ml. The detection mechanism is ascribed to a direct doping/de-doping of the active PEDOT:PSS film, where liposomes and liposome-based nanoparticles are pushed on its surface by the gate potential. Even though the much larger size of liposomes, results suggest that these particles could also penetrate into the polymer matrix, probably due to the quite soft and adaptable nature of these molecules. The time response of the devices for detection of L liposomes and LC nanoparticles is quite fast, taking 60 s to reach steady-state current. Furthermore, the devices can sense and discriminate successive injection of liposomes and liposome-based nanoparticles in real-time.

D. Eumelanin Sensing

Tarabella *et al.* [46] first reported an OECT-based biosensor to detect insoluble redox-active molecules. In particular, they developed a PEDOT:PSS-based OECT that can detect colloidal suspensions of synthetic eumelanin. Eumelanin is an insoluble biopolymer with central role in skin and eye photoprotection that can efficiently capture and quench damaging UV radiation and reactive oxygen species. Eumelanin sensing is based on the redox behavior of the polymer with the Pt gate electrode, similar to the sensing of hydrogen peroxide or dopamine reported with OECT devices operating in faradaic mode. The device exhibits a dynamic sensing range of 10^{-6} M – 10^{-2} M. In real-time monitoring mode, the sensor reacts almost instantaneously with a rapid relative change of the drain current (less than 3 s), and the sensitivity is improved down to the nanomolar range, with lowest detection limit of 10^{-9} M.

E. Gallic Acid Sensing

In general, polyphenols have great interest in food science applications due to their multiple health benefits. Gallic acid (GA) is one of the most important phenolic components in tea, grape and many other plants. GA is usually employed as a reference compound for the determination of total polyphenol content (TPC) in food, because of its strong antiradical activity and electrochemical oxidation effect. Recently, Xiong *et al.* [47] have developed high-sensitive, portable and disposable GA sensors using PEDOT:PSS-based OECTs. The sensing mechanism is based on the direct electro-oxidation of GA at the Au gate electrode. With the increase of GA concentration, the effective gate voltage increases, which in turn reduces the drain current (I_{DS}) of the OECT. The device performance was optimized by functionalizing the Au gate electrode with nanocomposites of a cation polyelectrolyte (poly(diallyldimethylammonium chloride) (PDDA)) and three carbon-based nanomaterials (CNMs): MWCNs, Gr and GO. CNMs can increase the sensitivity of the biosensors by increasing the electrocatalytic activity of the gate electrode. PDDA can attract GA molecules by electrostatic interaction, since they show the opposite charges in neutral PBS solution, and increase the effective concentration of GA near the gate electrode. The optimized sensor with MWCNT-PDDA modified Au gate shows a detection limit as low as 10 nM and works with high recovery for rapid and accurate assessment of TPC in real tea infusion samples.

F. Ascorbic Acid Sensing

Ascorbic acid (AA) or vitamin C plays a key role in many metabolic reactions, in pharmaceutical formulations and in food industry, due to its antioxidant properties. Gualandi *et al.* [48] developed a low-cost all-PEDOT:PSS OECT for AA sensing, based on the ability of this polymer to electrocatalytically oxidize AA, without any enzyme or other redox mediator. AA reacts with the conductive polymer at the gate electrode, increasing the gate current (I_G). This in turn leads to the extraction of charge carriers from the channel (de-doping), resulting in a decrease of the drain current (I_{DS}).

I_{DS} depends linearly on the logarithm of AA concentration in the range 10^{-6}-10^{-3} M. The performance of the device for optimized conditions (in terms of thickness and applied voltage), shows a detection limit equal to 10^{-8} M and a sensitivity of $(4.5 \pm 0.1) \times 10^{-6}$ A/decade.

Later, Zhang *et al.* [49] reported a highly-selective and sensitive OECT-based AA sensor with Au gate electrode modified with a Molecularly Imprinted Polymer (MIP) (Figure6d). MIPs are fabricated by molecular imprinting technique, which creates cavities that exhibit affinity for the selected template molecules in the polymer matrix. After the adsorption of AA and application of a positive gate voltage, the oxidation of AA occurs on the modified gate electrode, which permits the transfer of electrons near the electrode surface. This decreases the voltage drop at the gate/electrolyte interface, leading to the increase in the effective gate voltage that result in the decrease of the channel current. Under optimal conditions, this biosensor exhibits a low detection limit of 10 nM and a high sensitivity of 75.3 mA/decade channel current change. In addition, The MIP film considerably improves the selectivity of the sensor, owing to the specific recognition of the imprinted cavities. The MIP-OECT sensor shows excellent specificity to AA, preventing the interferences from other structurally similar compounds (aspartic acid, glucose, UA, glycine, glutathione, H_2O_2) and common metal ions (K^+, Na^+, Ca^{2+}, Mg^{2+}, Fe^{2+}). In addition, the applicability of this MIP-OECT was demonstrated in commercial vitamin C beverages.

G. Amino Acids Sensing

The group of Zhang extended the use of these novel MIP-OECT sensors to chiral detection of amino acids. Amino acids are important components in biological systems. Although L-amino acids have biological activity, the related D-forms may not be metabolized efficiently or can even result in unfavorable effects. Therefore, chiral recognition of amino acids becomes a very important concern. Zhang *et al.* [50] fabricated highly sensitive and highly selective chiral recognition biosensors for **D/L-Tryptophan** (D/L-Trp) and **D/L-Tyrosine** (D/L-Tyr) using MIP-OECTs. The MIP films can specifically recognize these enantiomers and can electrocatalytically oxidized Tpr and Tyr. Upon addition of L-Trp (L-Tyr), the cavities that are complementary to these molecules in size, shape and functional groups in the polymer matrix will be occupied through non-covalent interactions. In contrast, upon addition of D-Trp (D-Tyr), the imprint cavities cannot be filled. Moreover, when an appropriate voltage is applied to the gate, the L-Trp (L-Tyr) molecule will be oxidized to produce faradaic current, resulting in an increase in effective gate voltage, thereby reducing the channel current. The channel current decreases with increase in the analyte concentration. The devices feature a linear response range for L-Trp and L-Tyr from 300 nM to 10 μM, with sensitivity of 3.19 and 3.64 μA/μM, respectively. The detection limit for L-Trp was found to be 2 nM and 30 nM for L-Tyr. These devices also exhibit high selectivity towards different amino acids with similar structure.

Zhang *et al.* [51] also demonstrated the use of these MIP-based OECTs for the chiral detection of **D/L-Histidine**
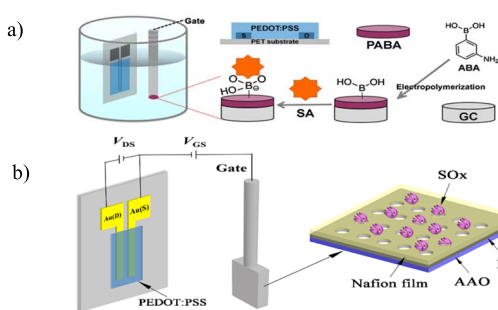
a)

b)

Fig. 7. a) Schematic of the principle for SA detection based on the OECTs with PABA-GC modified gate electrode (reproduced from [52] with permission from Elsevier, Copyright © 2017), b) Schematic diagram of an OECT-based sarcosine sensor with Nafion-SOx/Pt/AAo gate electrode (reproduced from [53] with permission from Elsevier, Copyright © 2019).

(D/L-His) (Figure6e). Although, D-His is not bioactive, L-His is an essential bioactive amino acid that plays a key role in several biological processes. Changes in channel current are proportional to D-His and L-His in the concentration range 100 nM-10 μM, with detection limits of 10 nM and 100 nM, respectively. The highly selective MIP film allows to differentiate L-His from D-His or D-His from L-His. This biosensor was also successfully used for L-His detection in human urine, demonstrating its feasibility for real applications.

H. Sialic Sensing

Sialic acid (SA) is a family of sugars that mediate or modulate many cellular interactions. Overexpression of SA on the cell membrane surface is characteristic of malignant and metastatic phenotypes for many types of cancers. Guo *et al.* [52] presented a novel OECT-based sensor for SA detection. The OECT consists of screen-printed carbon source and drain electrodes on flexible substrate, PEDOT:PSS active channel, and poly(3-aminophenylboronic acid) (PABA)-modified glass carbon (GC) gate electrode. The sensing mechanism is based on the selective interaction between phenylboronic acid group on the PABA/GC gate and the SA, without the need for any enzymatic or labeling processes (Figure 7a). The OECT is operated under non-faradaic regime. Therefore, the response of the OECTs to addition of SA is attributed to change of electrolyte solution potential (V_{sol}) acting on the PEDOT:PSS channel, resulting from the formation of the phenylboronic acid-SA complex. The phenylboronic acid-free SA interaction leads to the increase of the potential at the gate/electrolyte interface, which means the decrease of V_{sol}, and as result, the $|I_{DS}|$ increases with the addition of free SA. Under optimized conditions, the OECT device displays good performance for free SA sensing, with low detection limit equal to 8 μM, and linear response until 2.0 mM. In addition, the device has also the capacity to identify cancer cells (human cervical cancer, HeLa and HUVEC) from normal cells in a simple and non-invasive way. However, for the detection of cells, V_{sol} increases and as result the $|I_{DS}|$ decreases. Furthermore, compared to free SA, a longer time is needed to obtain stable I_{DS} for the monitoring of cells, which may be due to the slow

kinetic of the interaction between the phenylboronic acid and the cell membrane surface SA.

I. Sarcosine Sensing

Sarcosine is currently recognized as a potential non-invasive specific biomarker for prostate cancer. Recently, Hu *et al.* [53] have proposed a novel sensitive and selective OECT-based biosensor for sarcosine detection by integration of enzyme sarcosine oxidase (SOx), biocompatible polymer Nafion and nanomaterials (Anodized Aluminum Oxide (AAO)) on Pt gate electrodes (Figure 7b). The AAO increases the specific surface area of the gate electrode, SOx makes the detection both sensitive and selective by the biocatalytic reaction of sarcosine, and Nafion increases the selectivity of the sensor by promoting the enzyme immobilization and repelling negatively charged interferences. Consequently, the device with Nafion-SOx/Pt/AAO gate electrode shows excellent sensing performance. Sarcosine can be detected in a linear range from 50 nM to 100 μM, with a detection limit of 50 nM, well within the clinical range of prostate cancer levels in human urine (20 nM–5 μM). Sarcosine is detected by the indirect quantification of the oxidation of hydrogen peroxide (H_2O_2). The enzymatic decomposition of sarcosine by SOx produces H_2O_2 that is further oxidized on the surface of the Pt gate electrode. This results in electron transfer and faradaic current generation that changes the effective gate voltage and the channel current of the transistor. The selectivity of the biosensor is also significantly improved.

J. Multianalyte Sensing

Biosensors with multianalyte sensing capability are important for precise healthcare monitoring. Ji *et al.* [54] fabricated highly sensitive **glucose and lactate** OECT-based sensors by modifying Au gate electrodes with enzymes GOx and lactate oxidase (LOx), chitosan and pol(n-vinyl-2-pyrrolidone)-capped Pt nanoparticles (Pt-Ns). A polydimethylsiloxane (PDMS) microfluidic channel was integrated with the OECTs (Figure 8a-left), providing compact chip size sensors, short detection limit ($\sim$1 min) and very low consumption of analyte (30 μL). These individual OECT devices can reach a detection limit of glucose and lactate down to 10^{-7} M and 10^{-6} M, respectively. Multisensing is carried out by combining the glucose and lactate single sensors together with a dual microfluidic channel, for simultaneous detection of glucose and lactate (Figure 8a-right). This device can clearly differentiate the different glucose and lactate concentrations, proving that there is no crosstalk between the two individual sensors. This multiple sensor was successfully used to non-invasively detect glucose in human saliva, by previously adding negatively charged Nafion layer to the gate electrode, in order to eliminate UA and AA interferences.

The relatively high potential required for oxidation of H_2O_2 increases significantly interferences from endogenous electroactive species that are present in body fluids, leading to a decrease of the selectivity of the device. Moreover, the diffusion of H_2O_2 between nearby biosensors, in a single biological sample, can lead to electrical and chemical crosstalk, from
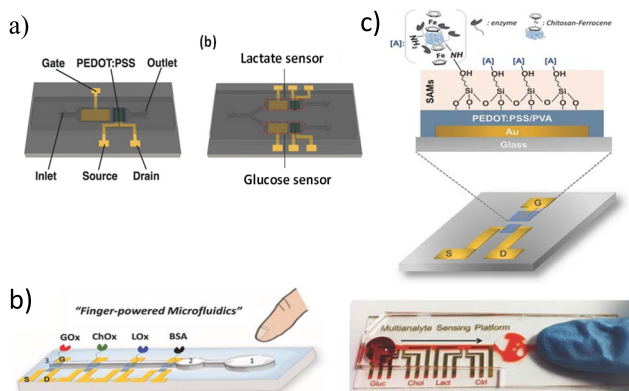
Fig. 8. a) Schematic diagrams of: (left) individual OECT-based sensor integrated with microfluidic channel, Au source/drain/gate electrodes and PEDOT:PSS active channel, and (right) OECT-based multianalyte sensor (reproduced from [54] with permission from John Wiley and Sons, Copyright © 2016), b) Biosensing multiplatform with the embedded "finger-powered" PDMS microfluidic showing (1) the activation button, (2) he liquid reservoir and (3) the punched inlet (reproduced from [55] with permission from John Wiley and Sons, Copyright © 2016), c) Schematic diagram of the OECT device structure and illustration of the biofunctionalization scheme at the gate electrode (reproduced from [55] with permission from John Wiley and Sons, Copyright © 2016).

capacitive coupling and H_2O_2 diffusion, respectively. An alternative to detection of H_2O_2 is the use of mediators to improve selectivity and performance. Pappa et al. [55] designed a compact multianalyte biosensing platform, composed of an OECT microarray integrated with a "finger-powered" microfluidic, for quantitative simultaneous detection of three key biomarkers: **glucose, lactate and cholesterol** levels (Figure 8b). They designed a novel biofunctionalization method that minimizes any background interference but it also provides selectivity towards specific metabolites. By incorporation of an electron mediator (ferrocene, Fc), molecular wiring of the enzyme active site was achieved, thus lowering the working potential of the electrodes, and reducing background signal (Figure 8c). By electrically isolating the individual devices, multi-analyte sensing is facilitated and electrical crosstalk between the different OECTs is avoided. The resulting biosensing platform was successfully used for real-time detection of a combination of analytes in human saliva samples, with high selectivity and sensitivity.

V. BACTERIA/VIRUS SENSORS

Food, water safety and disease control related to microbial pathogens, such as bacteria and/or viruses are extremely important to our daily lives. Conventional techniques require specialized laboratories and personnel, which is expensive and time-consuming. Several OECT-based bacteria sensors have been reported with LODs down to 100 cells/ml whilst virus sensors have shown, compared to other sensor technologies, very promising performances with LOD down to 0.025 HemAagglutination Units.

A. Bacteria Sensing

Specific types of bacteria in food or water can cause several life-threatening conditions. Enterohemorrhagic

Escherichia coli (E. coli) O157:H7 for example, is a widespread foodborne pathogen. He et al. [56] in 2012 successfully used a PEDOT:PSS-based OECTs with Pt or Ag/AgCl gate electrodes for the detection of E. coli in KCl electrolytes. In order to capture E. coli, anti-E. coli antibodies were attached using oxygen plasma treatment. It was found that when PEDOT:PSS was treated for 2 minutes with oxygen plasma, the capturing of E. coli was the highest and that even if PEDOT:PSS was treated for longer time, the density of the bacteria on the semiconducting layer did not change. Once bacteria are captured, the transfer curve of the OECT shifts to higher gate voltage. The authors claimed that this can be attributed to the electrostatic interaction between the PEDOT:PSS layer and the bacteria. It was further found that the voltage shift was dependent on the ion concentration of the electrolyte. In KCl concentrations higher than 10 mM, the negative charges on the bacteria were screened by electrochemical double layer and thus the device showed little response.

In 2014, Liao et al. [57] reported an OECT-based sensor for detecting **marine diatoms** in seawater. Diatoms are probably the first eukaryotic microalgae colonizing and dominating microcommunities in marine fouling. Once diatoms attach on the solid surface, they form diatom biofilms and cause the subsequent adhesion of many other fouling organisms. Adhesion of marine fouling organisms on artificial surfaces such as ship hulls will cause many problems, including extra energy consumption, high maintenance costs, and increased corrosion. Liao et al. studied the application of PEDOT:PSS-based OECTs in the detection of two species of common benthic fouling diatoms in the seawater medium for the first time. OECTs showed excellent biocompatibility and stable performance in seawater medium. The devices can be used to detect two typical diatoms: Navicula sp. and Amphiprore sp. (Figure 9a). The transfer curves of the OECT shifted to higher gate voltage after the capture of marine diatoms, which can be attributed to the electrostatic interaction between diatoms and the PEDOT:PSS layer. The devices can detect Navicula sp. and Amphiprore sp. concentrations as low as 100 cell/mL and 400 cell/mL, respectively.

In a more recent study in 2018 by Pitsalidis et al. [58], a P3HT-based OECT was demonstrated to detect **bacterial membrane disruption**. The OECT was used as a transducer of the permeability of a lipid monolayer at a liquid:liquid interface, designed to read out changes in ion flux caused by compounds that interact with and disrupt lipid assemble (Figure 9b). They demonstrated the concept using Polymixin B antibiotic and the highly sensitive quantitation of permeability of the lipid monolayer induced by two antibacterial amine-based oligothioetheramides. This platform is also able to assess the potency of such antimicrobial compounds.

In 2014, Tria et al. [59] reported an OECT for the dynamic monitoring of **Salmonella** typhimurium infection of polarized epithelia. The flow of ions across polarized epithelia is a tightly regulated process and hence, measurement of the transepithelial resistance is a highly relevant parameter for assessing the function or health of the tissue. Salmonella typhimurium and other enteric pathogens are well-known to disrupt ion flow in gastrointestinal epithelia. A PEDOT:PSS-based OECT
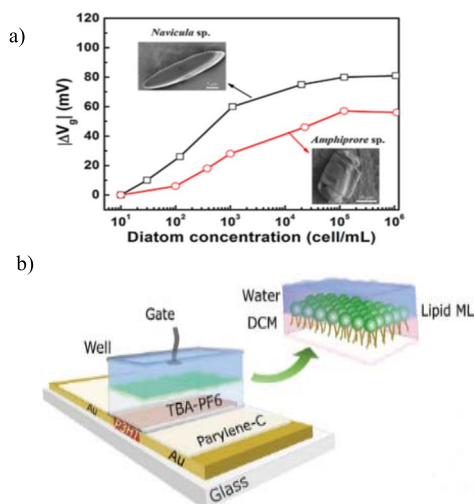
Fig. 9. a) Relative gate voltage shifts |₁Vg| of an OECT characterized at different diatom solutions with various concentrations (reproduced from [57] with permission from Elsevier, Copyright © 2014), b) Schematic structure of the biphasic–electrolyte gated OECT system (reproduced from [58] with permission from John Wiley and Sons, Copyright © 2018).
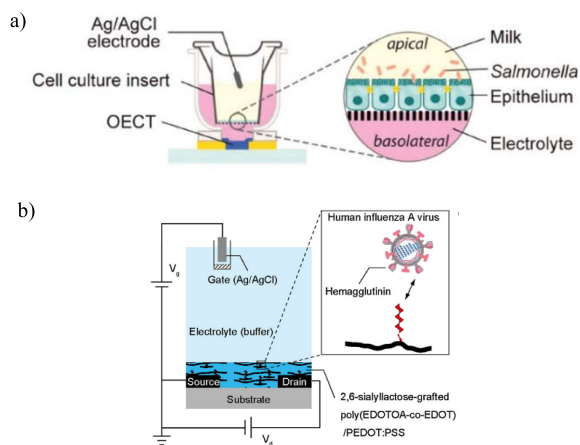

Fig. 10. a) Schematic diagram illustrating the integration of cells with OECT with milk in the apical side of the epithelial barrier (reproduced from [59] with permission from John Wiley and Sons, Copyright © 2014), b) Schematic cross section of the OECT with a thin layer of 2,6-sialyllactose-grafted poly(EDOTOA-co-EDOT)/PEDOT:PSS in an electrolyte (reproduced from [60] with permission from Elsevier, Copyright © 2018).

was integrated with epithelia to form the structure shown in Figure 10a. When a positive gate voltage was applied, cations from the electrolyte diffuse into PEDOT:PSS de-doping it, which decreases the source-drain current. It was deduced that the transient response described the ion flux between the gate electrode and the semiconducting channel hence, making it sensitive to the rate at which ions cross the barrier tissue layer. The devices demonstrated stable operation under physiological conditions and in dynamic, pathogen-specific diagnosis of infection of epithelia.

B. Virus Sensing

In 2018, Hai *et al.* [60] presented an OECT with a trisaccharide-grafted conductive polymer channel was used

to detect human **influenza A** virus in aqueous conditions using sialyllactose-functionalization (Figure 10b). In order to achieve highly sensitive, selective, and label-free virus sensing, a target recognition element was introduced into the electrochemical amplifier of the OECT. The drain current increased following virus adsorption onto the functionalized channel. LOD was more than two orders of magnitude lower (0.025 HemAagglutination Units (HAU)) than commercial immunochromatographic influenza virus assays, over the same detection time.

VI. CELL-BASED SENSORS

Cell-based biosensors monitor physiological changes in cells exposed to pathogens, pollutants, biomolecules or drugs. The use of OECTs on cell-based sensors has gained considerable interest due to its ability to act as a transducer of ionic signal to electronic current. Owing to the unique features of OECTs, they have been successfully used as cell biosensors to monitor cells-substrate attachment, cells confluence and barrier tissue integrity, transepithelial ion transport, cell stress and death, and cell surface biomolecules. The reported OECTs cell-based sensors have shown impressive temporal resolutions of down to 30 seconds for barrier tissue disruption compared to almost an hour from other reported sensors.

A. Cells Detachment

Yu *et al.* [61] first reported the use of PEDOT:PSS-based OECTs as cell-based biosensors. They showed that the OECTs display stable performance and excellent biocompatibility in culture medium. They successfully monitored in-vitro cell activity of human cancer cells (KYSE30) and fibroblast cells (HFF1) cultivated on the active channel of the OECTs. The devices are sensitive to morphological changes and cells detachment upon exposure to retinoic acid and trypsin. The sensing mechanism is attributed to the electrostatic interaction between the cells and the PEDOT:PSS active layer of the OECTs. The additional negative voltage applied by the cell on the OECT requires a higher gate voltage to compensate the effect of the attached cell.

B. Barrier Tissue Integrity

Barrier tissue in multicellular organisms serve as essential functional interfaces, by selectively controlling the passage of substances across the barrier: absorbing nutrients, electrolytes and water, while limiting the diffusion of ions, macromolecules, pathogens and other cells. Examples of barrier tissue in the body include epithelial and endothelial cells. Disruption or malfunction of the structures involved in transport through barrier tissue is often indicative of toxicity or disease. The ability of OECTs to conduct both electronic and ionic carriers makes it a promising device for interfacing with barrier tissue cells.

Jimison *et al.* [62] first showed the integration of OECTs with human cells for monitoring in situ barrier tissue integrity. Caco-2 gastrointestinal epithelium cells were grown on a Transwell membrane and incorporated into the OECT (Figure 11a). The cell monolayers act as a partial barrier to ionic current.
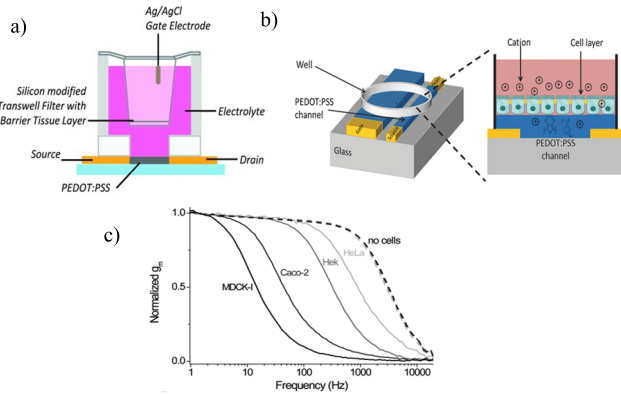
Fig. 11. a) Device architecture. The cell layer is grown on a Transwell filter and suspended between the gate electrode and the channel (reproduced from [62] with permission from John Wiley and Sons, Copyright © 2012), b) Device architecture. Cells and media are contained inside the well. The gate is located below the cell monolayer [65], c) Normalized transconductance (g_m◁ after 6 days incubation of MDCK-I, Caco-2, HEK and HeLa cells compared with the OECT without cells (dashed lines) (reproduced from [61] with permission from the Royal Society of Chemistry, Copyright © 2015).

In the presence of cells, the ion flux is decreased, slowing the OECT transient response. Thus, the channel current is a measure of the barrier function of the cells. They monitored in real time changes in the ionic flux after barrier tissue disruption induced by toxic compounds (ethanol and H_2O_2), with high temporal resolution (within only 30 seconds for H_2O_2 compared to 30-60 minutes reported in other studies [63]) and high sensitivity (in the range of 5-100 mM showing rapid response whilst at 1 mM the degradation proceeds slower). As result of the disruption of barrier tissue integrity, ionic transport across the cell layer increases leading to a faster OECT response. Later, they validated the ability of this OECT for assessing barrier tissue integrity by comparing it with traditional methods [64]. They showed that the OECT could measure disruption in barrier tissue with equal sensitivity for ethanol and greater sensitivity for H_2O_2 than traditional methods, due to inherent amplification from the organic transistor. The different nature of the response of these compounds is ascribed to the different molecular mechanism in inducing damage to barrier tissue. Furthermore, the OECT also exhibits increased temporal resolution due to its increased sensitivity to subtle breaches in barrier tissue.

However, the use of a top-gate device has certain limitations in fabrication and operation. To overcome these inconveniences, these authors developed a planar all-PEDOT:PSS OECT, compatible with low-cost production techniques, that can be used for simultaneous electronic and optical monitoring of epithelial cells in vitro, owing to the optical transparency of PEDOT:PSS [65]. The cells were cultivated directly into a well on top of the device that partially covers the channel and the gate (Figure 11b). Upon application of a positive gate voltage, the cell monolayer covering the channel reduces the flux of cations from the media to the channel. This results in slower de-doping of the channel and a change of the channel current. By measuring the OECT response, it is therefore possible to detect the ability of the cell monolayer to block

ion flow into the channel, and as consequence to assess the quality of the cell layer. This device was used to monitor growth and behavior of different types of epithelial cells (MDCK-I canine/HEK-293 human kidney cells, and Caco-2/HeLa human cancer cells), showing that the structures which regulate ion flow in these epithelial cells are functional before the cell monolayer is confluent. This demonstrates that the measured electrical signal is due to the barrier function of the cells rather than simple cell growth/coverage. The presence of cells on the active area of the OECT does not modify the transistor response unless the cells display barrier properties.

Later, they reported on the optimization of this planar OECT for barrier tissue sensing, in terms of gate choice, geometry, and improvement of cell adhesion [66]. First, different gate electrodes were tested to assess they biocompatibility and their ability to de-dope the PEDOT:PSS channel. Owing to their electrical performance and biocompatibility, PEDOT:PSS and Ag are suitable gate electrodes. Although Ag shows superior current modulation, the use of PEDOT:PSS has the major advantage that it facilitates the fabrication process. Moreover, by increasing the gate/channel area ratio, the current modulation can be improved. Next, the surface of the device was coated with different extracellular matrix (ECM) proteins, in order to improve cell adhesion on the PEDOT:PSS film. It was found that operation of the OECT is greatly improved by coating with fibronectin. Finally, the optimized OECT was successfully used to monitor disruption of barrier tissue of MDCK-I cells grown on the device, with increased temporal resolution compared to simultaneous optical monitoring.

In order to be competitive with commercially available impedance sensors for live-cell monitoring, these OECT-based sensors must be able to monitor not only barrier tissue but also coverage of any adherent cells on the active area of the device. Ramuz et al. [67] demonstrated that the OECTs have the ability to sensitively monitor different cell types over time, not only barrier tissue cells (such as MDCK-I and Caco2 cells), but also any adherent non-barrier cell type (like HeLa and HEK cells). The transistor performance was measured in terms of changes of transconductance with frequency. Results show that both tissue type cells are clearly distinguishable: barrier tissue cells are shown to have a more abrupt drop in transconductance compared to non-barrier tissue cells (Figure 11c). Furthermore, these devices are also compatible with high-resolution optical images in fluorescence mode, allowing continuous cell monitoring both electronically and optically.

More recently, Curto et al. [68] have demonstrated the coupling of OECTs with microfluidics. They have developed a microfluidic platform integrated with in-line electronic sensors based on OECTs. This platform can host cells in a more physiologically relevant environment (using physiologically relevant fluid shear stress, FSS), and allows for efficient multi-parametric in vitro cell monitoring. When cultured inside microchannels, the OECTs can monitor in real time changes in the cell layer capacitance and resistance, both under normal conditions and when exposed to toxins. This platform can also be used to monitor key metabolites uptake of the cells over time (like glucose uptake). Another important feature of this platform is the ability to carry out simultaneous optical

monitoring. In addition, a fully automated electrical wound-healing assay based on this platform was developed.

Recently, Yeung *et al.* [69] have investigated the potential effects of the OECT geometry on the performance and quality of cell-based sensing. They fabricated OECTs with different channel areas and incubated them with two epithelial cells separately (Caco-2 tight cells and NPC43 leaky cells). Although the different devices are able to detect local ion flux changes caused by epithelial cells, results show that there is a correlation between input frequency, size of the OECT channel and sensitivity of biological measurement. Given a range of transepithelial resistance, there exists an optimum bandwidth within which an OECT of particular size is most sensitive to. A large-channel OECT with elevated capacitance displays higher sensitivity to low frequency signals. Therefore, large-sized OECT is more suitable for measuring paracellular properties of tightly packed cells (like Caco-2 cells), that usually rely on low frequency current. On the contrary, a small-channel OECT performs better in capturing high frequency signals. Therefore, a smaller OECT is recommended for determining high frequency-related properties (like confluence and adherence) of leaky cells (like NPC43). Results from both the frequency and impedance analysis demonstrate that the sensitivity of the cell-based sensor is affected by the tightness of target cell and can be tuned by controlling the active area of the transistor.

C. Ion Transport

OECTs-based devices also offer a convenient way to monitor in situ transepithelial ion transport that occurs in epithelial cells of tissues and organs. Yao *et al.* [70] first reported direct coupling of cells physiological ionic current with OECTs. They showed the integration of human airway epithelial cells (Calu-3) with a PEDOT:PSS-based OECT array to successfully monitor activation and inhibition of transepithelial ion transport in real time through electrical readout. The cell monolayer was directly cultured on the OECT array surface. The sensing mechanism of this coupling is strongly dependent on the cation-sensitive properties of OECTs. By taking advantage of this property, the ion concentration change at the extracellular matrix region above the OECT surface due to transepithelial ion transport can be coupled to and reflected by the change of the channel current of the OECT.

D. Cell Death

Monitoring cell stress and death induced by drugs is an issue of great importance in toxicology, pharmacology and therapeutics. Romeo *et al.* [71] have developed a sensitive OECT-based sensor for direct in-vitro monitoring cell death. The device design was inspired by the architecture previously proposed by Yu *et al.* [61] by incorporating a Transwell membrane to the OECT in order to separate the ion detection from the ion drifting mechanism (Figure 12a). The gate electrode is immersed in a water layer between the membrane and the PEDOT:PSS channel, and is not directly in contact with the culture medium. Cell culture medium is confined in the Transwell support. When free area on the porous membrane
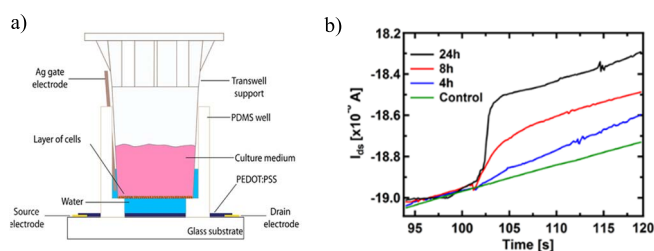

Fig. 12. a) Device architecture. The gate electrode operates in a thin layer of pure water that fills the small gap between the Transwell membrane and the PEDOT:PSS film (reproduced from [71] with permission from Elsevier, Copyright © 2015), b) Device dynamic response (IDS vs. time) upon exposure to 1 mM doxorubicin at different exposure times (reproduced from [71] with permission from Elsevier, Copyright © 2015).

becomes available, ions coming from the culture medium flow through the membrane into the underlying water. In this way, the driving force that causes ions flow through the membrane is the gradient of concentration that is practically not affected by the gate voltage but is in contrast only dependent on the surface of open pores. In addition, this configuration strongly reduces the deterioration of the PEDOT:PSS performance, typically induced by chemical processes when in direct contact with culture media or cells.

In order to monitor cells viability/death with this OECT-based device, human cancer cells (A549) were cultivated on the Transwell membrane. The cells grown on the membrane shields the drift of cations from the culture medium through the membrane pores into the underlying water. The increase ion density in the water layer depends on the available free area of the membrane. Once crossed the porous membrane, the gate voltage forces the cations to enter the PEDOT:PSS channel and de-dopes it, becoming the OECT sensitive to very small changes in ion concentration. Cells viability was studied upon exposure to the anticancer drug doxorubicin to a range of doses and times that fully covers the protocols used in cancer treatment. The change in the channel current I_{DS} could be directly correlated to the drug exposure time. When exposed to doxorubicin, the coverage of the Transwell membrane pores is reduced. Consequently, the flux of ions across the membrane increases, inseminating the water underneath and finally being detected by the OECT. On the other hand, the dynamic response as a function of the drug concentration indicates that the number of ions crossing the membrane strongly increases as the pores are cleared by the cells that dye (Figure 12b). Effects induced by doxorubicin could be detected down to 0.5 μM. The device efficiently monitors cell death dynamics, is able to detect signals related to specific death mechanisms, such as necrosis or early/late apoptosis. Furthermore, the OECT shows comparable response to standard cell viability/death assays, with higher sensitivity to the early stages of cell deterioration mechanisms and to apoptotic events.

E. Cell Surface Biomolecules

Cell surface glycoproteins play critical roles in diverse biological processes, including cell-cell communication, immunity, infection, growth, proliferation and differentiation.
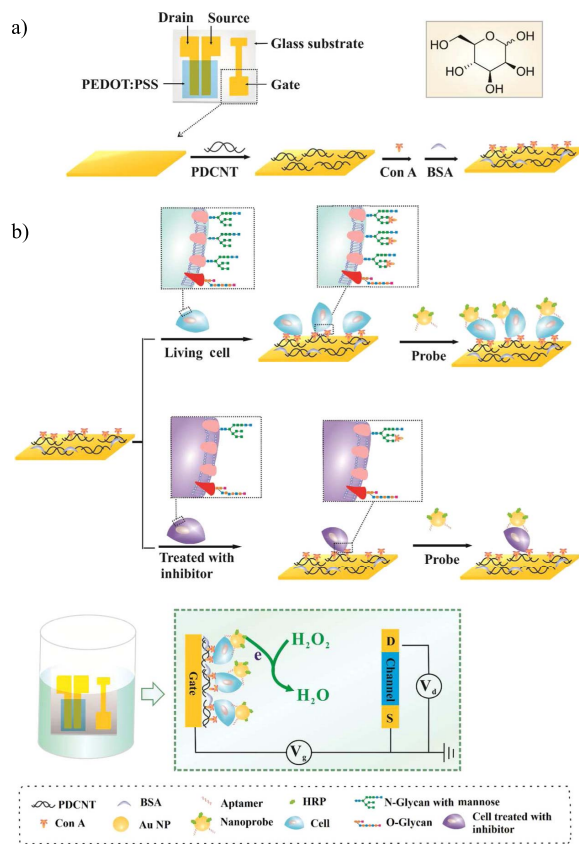
Fig. 13. a) Gate modification for mannose sensing (reproduced from [72] with permission from the American Chemical Society, Copyright © 2018), b) (up) Recognition of nanoprobes to the captured cancer cells by specific binding of the aptamer on the gold nanoparticles (Au NPs) to the cell surface and (down) electrochemical reaction at the gate electrode in PBS upon addition of H_2O_2 (reproduced from [72] with permission from the American Chemical Society, Copyright © 2018).

Their expressions are closely related to cancer growth and metastasis. Therefore, the dynamic monitoring of cell surface glycans can provide new insights into clinical diagnosis. Chen *et al.* [72] reported an OECT-based biosensor for the detection of glycans on living cancer cells. The device consists of a PEDOT:PSS active channel and a gold gate electrode modified with concanavalin A (Con A) loaded by carbon nanotubes (PDCNT) that can specifically bind to mannose, a glycan present on human breast cancer cells (MCF-7), and capture these cells (Figure 13a).

The number of capture cells is dependent on the amount of cell surface mannose. Since mannose is not electrochemically active, specific nanoprobes are introduced to the captured cells to produce an OECT signal. These nanoprobes are prepared by co-immobilizing the HRP peroxidase enzyme and an aptamer on Au nanoparticles (Figure 13b-up). The aptamer on nanoprobes can selectively bind to the MCF-7 cells surface, leading to an electrochemically active gate electrode because of the reduction of H_2O_2 catalyzed by the HRP enzyme conjugated on the nanoparticles (Figure 13b-down). The reduction of H_2O_2 can lead to a change of the effective gate voltage (V_g^{eff}) that results in a change of the channel current of the OECT. It is expected that more target cells

are captured on the gate electrode, more nanoprobes are loaded and thus a larger signal response is obtained. The current response increases with the increase of MCF-7 cells concentration, indicating that more target cells are attached to the gate electrode. The sensors can detect MCF-7 cell concentration down to 10 cells/μL. The OECT biosensor also shows good selectivity to mannose-expressed cells. The OECT signal is dramatically decreased upon exposure to N-glycan inhibitor due to the decrease of mannose expression on cells. Moreover, these biosensors provide a versatile platform for the analysis of other glycans and cancer cells by changing the binding lectin and the aptamer sequence.

VII. NUCLEOTIDE/IMMUNOSENSORS

Biomarkers in human samples like blood or serum exist at very low concentrations (nM-fM) making their detection and more importantly the changes in their concentration, a major challenge. OECTs are an attractive platform for such applications due to their very high transconductances. However, the investigation of immunosensors using OECT-based transduction to detect specific antibody–antigen (Ab–Ag) interaction remains sparse. On the other hand, DNA/RNA sensing based on OECTs has become a crucial technique to monitor concentrations of several nucleotide-based cancer biomarkers.

The reported performances of OECT-based nucleotide/immunosensors are extremely promising when combined with the low operating voltages, flexibility and biocompatibility. Although these devices have opened the doors for implantable devices, they fall behind in performance metrics like LODs, linear range, sensitivity and selectivity compared to other sensors. Reported LODs are in the range of several femtomolar and have linear ranges of up to 7 orders of magnitude. Other sensors based on silicon nanowires for example, have shown LODs down to the attomolar range with similar linear ranges. Nevertheless, silicon nanowire sensors operate at higher voltages and with more complicated electronic readout circuits compared to OECTs.

A. Immunosensors

Immunosensors, based on the highly specific molecular recognition of an antigen by antibodies, have become the major tools for clinical examinations, biochemical analyses of environmental pollutants and food quality control. In immunoassay, the determination of cancer markers associated with certain tumors plays an important role in diagnosing cancer diseases.

The **Prostate Specific Antigen**(PSA), an androgen-regulated serine protease, is the best serum marker currently available for the preoperative diagnosis and screening of prostate cancer. In a study from Kim *et al.* [73] in 2010, an OECT-based immunosensor was developed for PSA/1-antichymotrypsin (ACT) complex detection. This was achieved by the use of Au nanoparticles (AuNPs) conjugated with PSA polyclonal anti-body (pAb) where the AuNPs were used to amplify the signal (Figure 14a). The drain current increases linearly with PSA-ACT concentration to a sensitivity of 97 μA/log [PSA-ACT] due to the addition of the gold
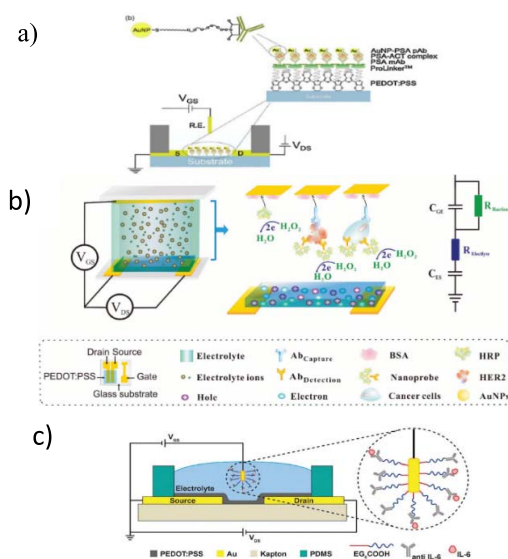
Fig. 14. a) Schematic illustration of the OECT-based immunosensor for the detection of PSA-ACT complex utilizing AuNPs for signal amplification (reproduced from [73] with permission from Elsevier, Copyright © 2010), b) Scheme of the OECT-based biosensor for the detection of a cancer cell protein biomarker HE1R2 (reproduced from [74] with permission from John Wiley and Sons, Copyright © 2017), c) Cross-sectional representation of the OECT-based immunosensor for the label-free and selective detection of IL-6 (reproduced from [75] with permission from the Royal Society of Chemistry, Copyright © 2018).

nanoparticles on the probes. The authors achieved a high sensitivity and a limit of detection down to 1 pg/ml, which is well below the cut-off limit of 4 ng/ml for the detection of PSA-ACT complex for hyperplasia and cancer.

In 2017, Fu *et al.* [74] reported another label-free immunosensor that could detect a cancer biomarker (**Human Epidermal growth factor Receptor 2**, HER2) several orders of magnitude lower than the detection limits of other electrochemical sensors. Figure 14b shows the design of the gate electrode of an OECT-based protein sensor. An Au gate electrode is modified with a specific HER2 antibody ($Ab_{Capture}$) that is used to capture HER2 proteins in solutions with high affinity and selectivity even in the presence of some interferences. The captured HER2 is subsequently modified with catalytic nanoprobes because HER2 proteins are not electrochemically active. The HPR enzyme catalyzes the electrochemical reaction of H_2O_2 in PBS and under a bias voltage, the redox current on the gate electrode is proportional to the amount of HPR on the surface of the electrode. The devices can specifically detect biomarker HER2 down to the level of 10^{-14} g/ml. The OECT sensors demonstrate responses to a wide range of HER2 protein levels, from 10^{-14} to 10^{-7}g/ml, which is sensitive enough to detect HER2 both in breast cancer cells and normal cells.

In 2018, Gentili *et al.* [75] reported another label-free, immunosensor using OECTs for the selective detection of **Interleukin-6**(IL-6), a vital cell signaling molecule in medicine and biology (Figure 14c). IL-6 was detected for concentrations down to its real physiological range, through the integration of an immuno-affinity regenerated cellulose (RC)

membrane on an OECT biosensor. This improved the detection limit of the device, due to the fact that the capturing membrane increases the effective concentration of IL-6 interacting with the OECT by one order of magnitude. Additionally, the gate/electrolyte interface was investigated for selectively in detecting IL-6 via the immobilization of anti IL-6 antibodies onto the surface of the gate electrode. They also showed that the use of oligo(ethylene glycol) (OEG)-terminated self-assembled alkanethiolate monolayers (SAMs) for the immobilization of antibodies prevents non-specific protein binding, which is one of the major limitations to selectively detect IL-6.

It is worth noting here that the approaches used for immunosensors and cell surface biomolecules shown in Figure13 & Figure 14 are very similar. It is interesting that in most cases, the gate electrode is the one chosen to be functionalized, especially in situations where the expected effect is capacitive, since it will affect the de-doping mechanism of the conductive polymer used. However, in the case of Kim *et al.* the conductive polymer itself was functionalized because the expected result was to directly affect the inherent properties and the de-doping mechanism of the conductive polymer.

B. Nucleotide Sensors

The detection of biomarkers for several diseases, such as cancer biomarkers, using biosensors has attracted a lot of attention. Among them, OECT-based sensors for nucleic acids diagnosis has attracted much interest due to their ease of use and low cost.

Lin *et al.* [76], in 2011 reported the first OECT-based **DNA sensor** integrated in flexible microfluidic systems. Label-free DNA sensors were developed using PEDOT:PSS-based OECTs, in which single-stranded (ss) DNA probes were immobilized on the surface of Au gate electrodes (Figure15a). These devices can be used to detect complementary DNA targets at concentrations as low as 1 nM. The detection limit of the DNA sensor is extended to 10 pM when the hybridization of DNA is enhanced by applying an electric pulse to the gate electrode in the microfluidic channel. The sensing mechanism of this type of DNA sensor is attributed to the modulation of the surface potential of the gate induced by the immobilization and the hybridization of DNA molecules on this electrode.

Later, Tao *et al.* [77] reported a similar DNA sensor using complementary DNA (cDNA) as a probe and a nanoporous Au gate. A peptide nucleic acid (PNA) probe was used and adapted for DNA sensing due to its higher sensitivity and specificity. The offset gate voltage of the sensor is related to the potential drop at the intefaces of the gate electrode and the semiconducting channel. The voltage shift is saturated at high concentrations (> 15 nM) but steadily declines for lower concentrations. The linear range for cDNA is from 0.5 nM to 12.5 nM. Due to the higher specificity of the PNA probe and the higher sensitivity of the nanoporous Au gate electrode, one-base mismatch and two-base mismatch DNA sequences could be discriminated. There was no distinguishable response from the device between a three-base mismatch DNA sequence and a fully random sequence.
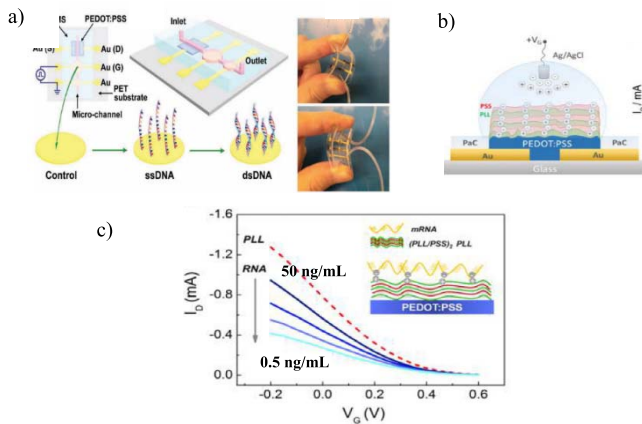
Fig. 15. a) Schematic diagram of an OECT-based DNA sensor integrated in a flexible microfluidic system (reproduced from [76] with permission from John Wiley and Sons, Copyright © 2011), b) Schematic representation of an LbL modified channel of an OECT (reproduced from [78] with permission from the American Chemical Society, Copyright © 2017), c) Change in transfer characteristics of the LbL modified OECT upon addition of increasing concentrations of mRNA (reproduced from [78] with permission from the American Chemical Society, Copyright © 2017).

In the same year, Pappa *et al.* [78] reported a novel functionalization approach on a PEDOT:PSS-based OECT. They demonstrated the deposition of oppositely charged polyelectrolyte multilayers (PEMs) in a layer-by-layer (LbL) assembly, thus combining the advantages of well-established PEMs with a high-performance electronic transducer (Figure15b). This technique is highly versatile and enables fine-tuning of crucial film parameters such as thickness and rigidity. Moreover, PEMs affect the injection of ions into the channel and further modulate the electrical potential in the electrolyte. This PEMs capability was utilized as a strategy to sense charged biological species, such as **mRNA**. The LbL-modified OECTs are able to sense nucleic acid in the electrolyte with a high sensitivity within a broad linear range at low operating voltages (Figure15c). These devices are able to detect the presence of mRNA at physiologically relevant salt concentrations.

In 2018, Peng *et al.* [79] showed the use of OECTs for miRNA-21 sensing. They fabricated a screen-printed OECT on a flexible PET substrate with carbon source and drain electrodes and modified AuNPs gate electrode. The use of AuNPs significantly increases the sensitivity in the range of 5pM to 20nM with a detection limit as low as 2 pM.

VIII. ELECTROPHYSIOLOGICAL SENSORS

OECTs are the focus of intense development for applications in bioelectronics owing to their large transconductance among electrolyte-gated transistors. For biointerfacing, the transconductance quantifies the "efficiency" of transduction of a biological event. At the same time, OECTs can achieve a response time well below a millisecond, sufficient for most biosensing applications. Therefore, OECTs make powerful amplifying transducers in biological applications, including recordings of brain and heart activity and electrochemical detection of neurotransmitters.
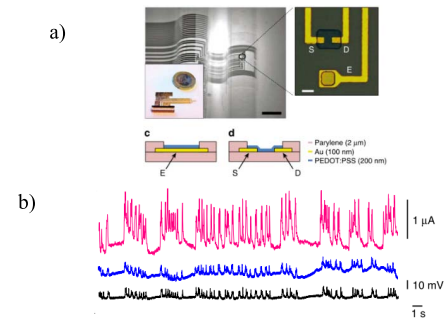

Fig. 16. a) Optical micrograph of the probe conforming onto a curvi-linear surface (reproduced from [80] with permission from Springer Nature, Copyright © 2013), b) Recordings from an OECT (pink), a PEDOT:PSS surface electrode (blue) and an Ir-penetrating electrode (black). The transistor was biased with VD = 0.4V and VG = 0.3V (reproduced from [80] with permission from Springer Nature, Copyright © 2013).

This is probably the most promising sensing application of OECTs. Owing to their very high transconductance, flexibility, fast enough response, low cost and biocompatibility, their use for the recording of electrical signals from either the brain or the heart or any other part of the human body, has received an exponential attention from researchers all of the world. They have exceeded the performances of other electrophysiological sensors with SNR values of up to 52 dB. It is predicted that OECT-based electrophysiological sensors together with possibly wearable and textile sensors, will grow much faster and form a major part of the industry in the coming years.

A. Brain Activity

One of the most common techniques to understand the basic mechanisms of processing information in the brain is to implant or attach metal electrodes on the surface of the brain. State-of-the-art recordings are currently being performed using microfabricated arrays, capturing the local field potentials, which are generated by the spatiotemporal summation of current sources and sinks in a given brain volume. Since OECTs capture ion fluxes, they are ideal to measure electrophysiological signals, which are fluctuations of the electric field generated by the movement of ions. Additionally, OECTs are cytocompatible and can be integrated on flexible substrates making them attractive candidates for neural interfacing.

In 2013, Khodagholy *et al.* [80] reported the use of OECTs for in vivo recordings of electrophysiological signals on the surface of the brain. Highly conformable arrays of OECTs were fabricated (Figure 16a) and used to carry out electrocorticography on the cortex of rats. Voltage signals were picked up by the gate electrode, changing the transconductance of the OECT, which in turn changed the drain current. Due to the high transconductance, the devices could detect low signals with high signal-to-noise ratio. Compared with surface electrodes, OECTs showed a superior signal-to-noise ratio due to local amplification (Figure 16b). These devices were able to record richer electrophysiological signals, similar to those obtained with penetrating electrodes.

Later, the same group demonstrated the importance of fabrication parameters on the performance of the OECT,

especially for electroencephalography (EEG) recordings [81]. The channel thickness can be used to tune the transistor performance to fit the specific application of EEG recordings. It was found that the uptake of ions from an electrolyte into a PEDOT:PSS film leads to a purely volumetric capacitance of 39 F/cm^3, hence the transconductance was depended on channel thickness.

B. Heart Activity

Electrocardiography (ECG), used to monitor and real-time treatment of several cardiac diseases, has become a well-established field for the application of electrical devices, such as implanted pacemakers. Despite the plethora of knowledge in this field, new generations of implantable devices are needed that combine the possibility to interface with bioelectric activity and minimize the invasiveness during implantation, operation and possible removal.

In 2014, Campana et al. [82] reported a PEDOT:PSS-based OECT fabricated on a poly(L-lactide-co-glycolide) (PLGA) substrate to be used for electrocardiographic recording (Figure 17a). PLGA is generally considered a resorbable bioscaffold that can be used for implantable biomedical devices. They successfully demonstrated a structure that combines biocompatibility and biodegradability with excellent electronic properties for fast and sensible potentiometric sensing in aqueous conditions. The quick ion-to-electron exchange, a crucial feature for bioelectric interfaces, stems from the intrinsic properties of the PEDOT:PSS layer. The sensing voltage at the gate was converted to drain currents by changing the transconductance of the device. By optimizing the layer thickness and the channel geometry, sensing signals could be detected down to a few tens of microvolts at timescales of a few milliseconds (1.5 ms). As a medically relevant bioelectric recording device, the transistor was applied in electrocardiography and showed a signal-to-noise ratio that is comparable to that of standard faradaic electrodes (Figure 17b).

In 2016, Gu et al. [83] demonstrated a 16-channel OECTs array for mapping the propagation and studying the characteristics of action potentials of primary cardiomyocytes in vitro. Primary neonatal rat cardiomyocytes were directly cultured on OECT coated with fibronectin with varied cell density. The OECT was based on PEDOT:PSS and gold electrodes. The physiological activities of a rat cardiomyocyte monolayer during a long-term culturing were revealed by this biocompatible, low-cost, and high transconductance OECT. The important parameters in studying cardiac electrophysiology (such as heart beat frequency, direction and velocity of the propagation of action potentials, action potential duration, and action potential rise time) could be obtained to quantitatively describe the action potential characteristics. The long-term monitoring capability of the OECT array was also well demonstrated. With the ability of mapping the action potential in a 2D scale, it was able to reproduce the irregular action potential propagation on a rat cardiomyocyte model.

Hempel et al. [84] in 2017 also used OECTs arrays to monitor the electrophysiological activity of cardiac cells. They developed OECT devices in a wafer-scale process and used
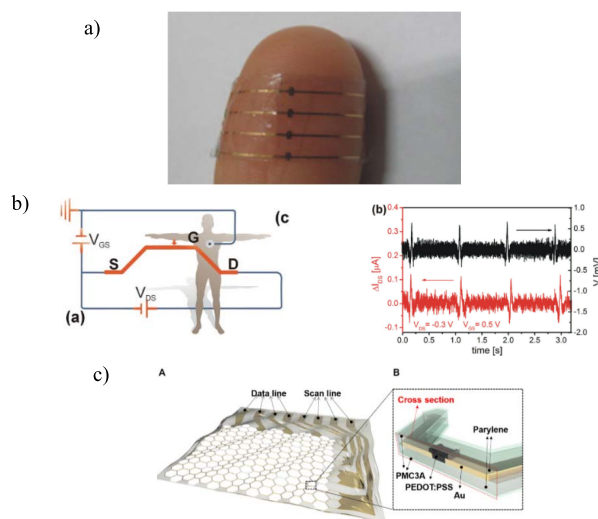

Fig. 17. a) Photograph of the device showing its transparency and adaptability when attached to human skin (reproduced from [82] with permission from John Wiley and Sons, Copyright © 2014), b) Measured drain current trace (red) as obtained during ECG recording with the OECT operated in direct contact with the skin (VSG=0.5V, VSD= −0.3V) and comparison to a normal potentiometric recording with standard disposable leads (black) (reproduced from [82] with permission from John Wiley and Sons, Copyright © 2014), c) Stretchable OECT array on honeycomb grid substrate [85].

them as electrophysiological biosensors measuring electrophysiological activity of the cardiac cell line HL-1. They demonstrated a high signal-to-noise ratio of up to 8 with significant cell signals, along with a small noise in the range of only 100–200 μV (peak-to-peak). However, the sensitivity degraded after repetitive measurements over 20 minutes. Their optimized devices showed very promising properties such as the ability to record fast components of extracellular signals. Combined with an easy, cost effective fabrication and the transparency of the polymer, this platform offers a valuable alternative to traditional systems.

In a more recent study, Lee et al. [85] reported an active multielectrode array-based on OECTs that simultaneously achieves nonthrombogenicity, stretchability and stability (Figure 17c). Hence, allowing the long-term ECG monitoring of the dynamically moving hearts of rats, even with capillary bleeding. The measured ECG signals have a high signal-to-noise ratio of 52 dB due to the active data readout.

IX. WEARABLE SENSORS

Selective detection of bioanalytes in physiological fluids (like blood, sweat and saliva) is of crucial importance in diagnosis and prevention for healthcare applications. Moreover, in-situ monitoring of physiological molecules (like glucose, lactate and saline concentration) allows opportunities in fitness. Wearable sensors are a promising solution for a novel class of point-of-care devices for in-situ and real-time physiological monitoring that could be extensively and easily integrated into the daily life in the form of non-invasive body sensors. OECTs can be integrated into efficient wearable sensors owing to their unique features: they directly amplify the electrochemical signal, their readout electronics is simple,
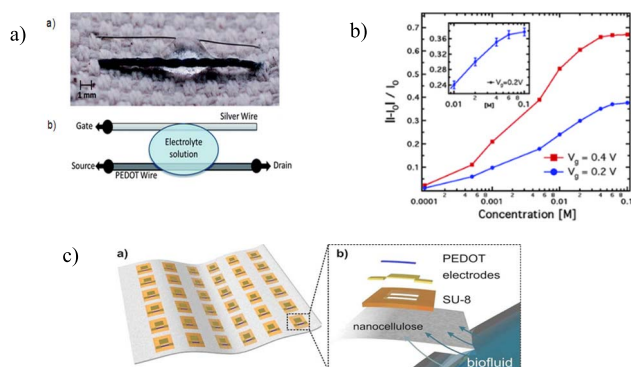
Fig. 18.   a) Cotton-based OECT directly integrated on cloth(reproduced from [86] with permission from the Royal Society of Chemistry, Copyright ©2012), b) Normalized response of the cotton-based OECT as a function of NaCl concentration at different gate voltages(reproduced from [86] with permission from the Royal Society of Chemistry, Copyright © 2012), c) Illustration of the biolectronic decal. Multiple OECTs can be fabricated on one ultrathin (<20 mm) cellulose sheet [87].

and they allow for very low power supply and portable devices. Simple solution-based processing techniques allow to easily obtain wearable OECT sensors in the form of flexible and implantable devices or electronic textiles. Implantable devices can be fabricated by directly printing the OECT on a flexible substrate, using techniques (like screen-printing) that are widely used in the textile industry and can be easily scaled to industrial processes. On the other hand, OECTs can also be directly integrated in textile fabrics. Different strategies for the functionalization of textile fibers (mainly cotton and nylon yarns) have been successfully used to obtain conductive fibers that can be woven in conventional looms. Owing to these unique features, wearable OECT sensors have demonstrated to be the state-of-the art platform for point-of-care testing of biomarkers in physiological fluids: ions, alcohol, lactate, neurotransmitters, amino acids, glucose, hormones, etc.

A. Ion Sensing

The sensitive and selective detection of ionic species in aqueous solution is of great importance for healthcare applications. For instance, sweat sodium concentration is generally related to the heart rate and Na^+ imbalance in sweat is generally related to dehydration. Tarabella *et al.* [86] fabricated an OECT-based device directly integrated in a textile for monitoring **saline content.** They used a natural cotton fiber and functionalized it with PEDOT:PSS by a simple soaking process. This conductive cotton thread was used as the transistor channel, directly interfaced with a liquid electrolyte in contact with a silver (Ag) wire gate electrode (Figure 18a). This cotton-based device has demonstrated to be very effective for electrochemical sensing of NaCl concentration in aqueous solution. The sensing mechanism relies on the redox reaction between Cl^- ions in solution and the Ag gate electrode. The OECT shows a stable and reproducible current modulation and displays an increasing modulation signal over all the NaCl concentrations investigated (Figure 18b). Gate voltage modulation is effective even at low voltages ($V_G = 0.2$ V). Modulation is also clearly distinguishable in the physiological

range of Cl^- concentration in sweat (30-60 mM), suggesting potential application of this wearable device for salt sensing in healthcare and fitness.

More recently, Yuen *et al.* [87] have reported a flexible, ultra-thin and self-adhering bioelectronic decal for epidermal electronics that can collect, transmit and interrogate a biofluid (*e.g.* sweat, saliva). The device integrates a PEDOT:PSS-based OECT as the sensing component, with an ultrathin microbial nanocellulose membrane, as the sampling holding component (Figure 18c). The decal is biocompatible and its entire thickness is less than 25 μm, which enables safe conformational adherence directly onto human skin. The porous and hydrophilic nanocellulose substrate is permeable to liquids and gases, thus allowing the efficient vertical wicking of biofluids secreted by the skin and their transport to the sensing electronics on top. This approach provided physical isolation of the electronics whilst enabling efficient biofluid delivery to the transistor. The bioelectronics decal displays high-currents and on-off ratios. The measurement range of the device falls well within the NaCl concentration range in human sweat. The OECT decal exhibits excellent performance with sensitivity to NaCl as low as 17.1 μM. The sensing mechanism is based on the de-doping of the active PEDOT:PSS layer by Na^+ cations, with a resultant drop in conductivity. The device repeatability depends on the printing quality, so its performance can be easily and substantially improved with optimization of printing conditions and ink selection. Furthermore, functionalization of nanocellulose is able to widen the variety of analytes, which can be electrochemically sensed using similar bioelectronic decals.

On the other hand, the sensitive and selective detection of **heavy metal ions** in aqueous solution is also of great importance for healthcare diagnosis. Thus, a very low level of lead ions (Pb^{2+}) can induce severe damage to the brain and central nervous system because of its potential bioaccumulation and toxicity. Wang *et al.* [88] reported a fiber OECT for monitoring lead ions. The OECT is based on nylon fibers modified with PVA-co-PE nanofibers (NFs) and conductive polypyrrole nanowires (PPy). Introduction of nanofibers increases the sensitivity of the sensor, owing to the high surface-to-volume ratio and the enhanced carriers transport ability. The PPy/NFs/Nylon fibers were integrated with PVA and HCl solid state electrolyte. The channel of the OECT is defined by the overlap of the solid electrolyte with the area of the source-drain fiber. As a result, the device is a fully solid and flexible sensor. This fiber-based OECT exhibits remarkable electrical performances, on/off ratios of up to 10^4 and applied voltages even below 2V. This device can efficiently detect lead cations in aqueous solution, in the 10^{-5}-10^{-2} M concentration range. The transfer curves of the OECT shift to lower gate voltage with increasing Pb^{2+} concentration. Furthermore, the channel current can be modulated by applying different gate voltages, which further enhances the sensitivity of the sensor. This fiber OECT exhibits good sensitivity to Pb^{2+} ions of 446 μA/decade with a low detection concentration of 10^{-5} M. The sensing mechanism is ascribed to the de-doping process of the active layer: by application of a positive gate voltage, Pb^{2+} cations are injected into the PPy

layer, leading to a decrease of the number of charge carriers and the channel conductivity. Application of a positive gate voltage results in the transition between the PPy oxidized state to the neutral state, according to the following electrochemical reaction:

$$n\left(PPy^+{:}NO_3^-\right) + M^{n+} + ne^- \leftrightarrow nPPy^0 + M^{n+}{:}NO_3^- \tag{6}$$
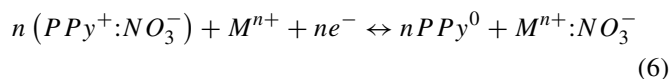
where M^{n+} refers to the cation from the electrolyte (analyte), n is the number of cation charge, and e^- represents the electron transported inside the PPy active layer.

As consequence, the channel current decreases as the lead ions concentration increases. In addition, the ion selectivity of this fiber OECT was investigated in aqueous solutions of different cations: K^+, Ca^{2+}, Pb^{2+} and Al^{3+}. The device shows great difference in the response curves to different cations, revealing very good selectivity to Pb^{2+} against other metal ions.

B. Alcohol Sensing

A breathalyzer measures the concentration of ethanol in the breath to estimate the Blood Alcohol Concentration (BAC) of an individual. The development of an easy-to-use, inexpensive, disposable and wearable breathalyzer would greatly simplify real-time BAC monitoring. OECTs are excellent candidates for disposable and wearable biosensors since they can be rapidly and inexpensively manufactured by printing techniques (screen-printing, inkjet printing) on flexible substrates. Bihar *et al.* [89] designed a proof-of-concept disposable breathalyzer using a PEDOT:PSS-based OECT printed on paper as the sensor. Alcohol deshydrogenase (ADH) and its cofactor nicotinamide adenine dinucleotide (NAD^+) were immobilized onto the OECT channel with an electrolyte collagen-based gel, making the device robust and easy to use. When the OECT-breathalyzer is exposed to ethanol, the enzymatic reaction of ADH and ethanol transforms NAD^+ into the reduced form NADH, and oxidizes ethanol into acetaldehyde:

$$CH_3CH_2OH + NAD^+ \xrightarrow{ADH} CH_3CHO + NADH + H^+ \tag{7}$$
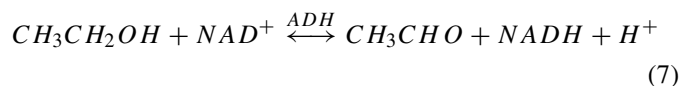
Then, NADH reduces itself according to:

$$NADH \rightarrow NAD^+ + H^+ + 2e^- \tag{8}$$
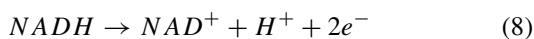
The electrons produced by NADH oxidation are collected by the gate electrode, causing a shift of the applied gate potential to the channel/electrolyte interface, which leads to a decrease in the OECT source-drain current (I_{DS}). Since the NADH concentration is directly related to the ethanol concentration in breath, the decrease in I_{DS} can be used as the output signal for quantitative detection of ethanol. This OECT-breathalyzer detects ethanol in solution for concentrations as low as 0.0004%. Preliminary breath alcohol tests for BAC detection with limited human volunteers were also conducted. This OECT-breathalyzer can detect ethanol in the breath equivalent to BAC from 0.01% to 0.2% with a performance comparable to that of a commercial breathalyzer.
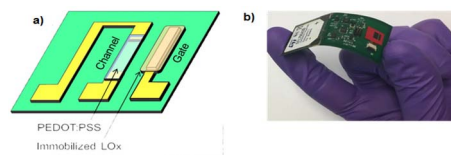

Fig. 19. (left) Schematics of the OECT for sensing lactate in sweat and (right) flex board implementation [90].

C. Lactate Sensing

Lactate is an essential analyte in physiological measurements that provides a biochemical indicator of anaerobic metabolism. During physical exercise, lactate concentration increases, making it a useful parameter to monitor wellness, physical fitness and the exercise effects. Lactate can be found in blood and sweat, although its detection in sweat offers a less invasive and dynamic way, particularly during exercise. Khodagholy *et al.* [90] reported the use of PEDOT:PSS-based OECTs as wearable biosensors for lactate detection. They developed a fully solid state yet flexible sensor for lactate monitoring in sweat that uses an ionogel as solid-state electrolyte. Ionogels are solid or gel-like polymeric materials that are made of room temperature ionic liquids (RTILs) with structure and dimensional stability. The ionogel is also used here to immobilize lactate oxidase (LOx) enzyme and the ferricenium (Fc) mediator. Upon introduction of lactate, the analyte is oxidized to pyruvate, while LOx is reduced and cycles back by the Fc/Fc$^+$ couple, which carries electron to the gate. This leads to a decrease in the potential across the gate/electrolyte interface and subsequent increase in the potential at the channel/electrolyte interface. As a result, more cations from the electrolyte enter the channel and de-dope it, leading to an increase in the modulation of the drain current. The OECT sensor can detect lactate in the physiological range (10-100 mM), including the relevant range of lactate in sweat.

More recently, Currano *et al.* [91] have reported a complete wearable sensor system for non-invasive detection of lactate in sweat. The device consists of a thin, flexible Kapton patch (2.5 × 7.5 cm) with on board power (lithium-ion battery) and controlling electronics that can collect, store and transmit data. The system can be coated with an adhesive and affixed to the skin. The transducing element is an OECT that can be easily removed and replaced due to saturation or aging (Figure 19). The sensor system can be controlled by a cell phone and the data can be downloaded and displayed in a smartphone app. A PEDOT:PSS-based OECT functionalized with lactate oxidase (LOx) is used in this system for monitoring the lactate concentration in sweat. Optimization of the sensor performance was reached when using a Pt gate electrode coated with LOx immobilized in glutaraldehyde with bovin serum albumin (BSA). In the presence of lactate, the enzymatic reaction of the analyte with LOx produces H_2O_2, which is then reduced by Pt. The gate electrode donates electrons in this process, increasing the effective gate potential. As a result, mobile ions in the electrolyte enter the channel and de-dope it, reducing its conductivity. Consequently, as the concentration of lactate increases, the drain current of the sensor decreases. The time
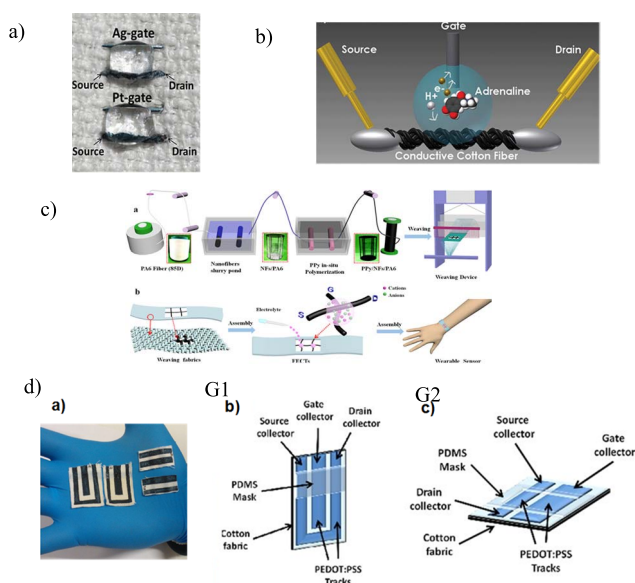
Fig. 20. a) OECT sensor system directly integrated on cloth for selective detection of adrenaline (reproduced from [92] with permission from the Royal Society of Chemistry, Copyright © 2014), b) Schematic of the cotton-based OECT with Pt-gate electrode and an adrenaline molecule in its sensing process (reproduced from [92] with permission from the Royal Society of Chemistry, Copyright © 2014), c) (up) Preparation process and weaving of the fibers. Polypyrrole (PPy) is in-situ polymerized onto the polyamide (PA6) fibers coated with PVA-co-PE nanofibers (NFs) and (down) assembly of the woven OECTs as wearable DA sensor (reproduced from [93] with permission from the American Chemical Society, Copyright © 2019), d) Screen-printed OECTs fabricated with two different geometries: G1 and (reproduced from G2 [94] with permission from Springer Nature, Copyright © 2016).

response to changes in lactate concentration is on the timescale of several minutes. While the sensitivity of the OECT is very good, the sensor exhibits saturation at lactate levels above 1 mM. Saturation of the sensor appears to be limited by reaching a maximum rate in either the enzymatic reaction or catalytic reaction at the gate. This sensing platform can be expanded to multiple analytes, with potential application in health and fitness monitoring.

D. Neurotransmitter Sensing

Adrenaline plays a central role in many instinctive responses, especially under stress and strong physical conditions. Real-time detection of abnormal adrenaline concentration could be a fingerprint of a pathological situation. In sports, adrenaline sensing can be useful to monitor physiological performance during training and competition of athletes. Coppedè *et al.* [92] designed an innovative textile sensor system for selective detection of adrenaline with respect to saline content in human physiological fluids. The OECT sensor was fabricated by integrating two cotton-based OECTs [86] on the same fabric patch, one with a Ag gate electrode and the other with a Pt gate electrode (Figure 20a). The two OECTs are very close to each but work independently, giving the opportunity to detect simultaneously and independently different analytes: the Ag-gate OECT is sensitive to saline content, while the Pt-gate OECT is sensitive to adrenaline. The sensing mechanism

involved in the detection of adrenaline is based on the oxidation of adrenaline to adrenaline-quinone and to adrenochrome at the surface of the Pt-gate electrode. As a result, a faradaic current is generated in the source-gate circuit and H^+ ions are released in the solution, de-doping the PEDOT:PSS active layer (Figure 20b). Under the faradaic regime of operation, the potential drop at the electrolyte/gate interface decreases and the effective gate voltage (V_g^{eff}) increases, forcing H^+ cations to move to the channel and de-dope PEDOT:PSS. This biosensor has been demonstrated to detect adrenaline selectively, compared to the saline content in human physiological fluid. Real-time measurements have been performed using human sweat as electrolyte and monitoring the device response (I_{DS}) upon injection of adrenaline, confirming that this is readily measurable using the Pt-gate electrode, while it is negligible with the Ag-gate electrode. Moreover, it was also demonstrated that adrenaline sensing is completely independent from saline content sensing.

Dopamine (DA) level detection in extracellular fluids or biological systems with excellent sensitivity, selectivity and fast response is of vital importance. Recently, Qing *et al.* [93] have developed a fiber-based OECT fully integrated in fabric for DA sensing. The OECT was based on polyamide fibers (PA6) coated with PVA-co-PE nanofibers (NFs)/polypyrrole (PPy) nanofiber network [88].This device unit can be directly integrated into a plain weave fabric product by traditional loom (Figure 20c). These PPy/NFs/PA6-based OECTs exhibit outstanding electrical performance, such as large on/off ratio up to 10^2, short response time of 0.34 s, and good cycle stability. The current amplification ratio and response rate of these devices notably outperform traditional OECTs. The DA sensing mechanism relies on the electro-oxidation of DA at the gate electrode according to the following chemical reaction:

$$DA \leftrightarrow o - dopamine\ quinone + 2H^+ + 2e^- \qquad (9)$$

This oxidation of DA at the gate increases the electrolyte potential according to the Nernst equation, which decreases the potential drop at the electrolyte and gate interface, and in turn results in the increase of the potential drop at the electrolyte and channel interface. Consequently, the channel current decreases as DA concentration increases. Compared to metal gate electrodes, the fiber gate electrode has shown to have larger initial channel current, superior sensibility (even when DA concentration was decreased to 1 nM), shorter response time (within 0.5s), higher sensitivity (47.28 NCR/decade), better repeatability and outstanding selectivity against interferents dominant in body fluids at higher concentrations than DA (NaCl, UA, AA and glucose). All these merits suggest that the all-PPy/NFs/PA6 OECT system can potentially be applied for sensitive and selective DA sensing.

Gualandi *et al.* [94] developed a fully textile, wearable sensor for real-time detection of redox active biomolecules. The sensor is based on an all-PEDOT:PSS OECT that was screen-printed on a cotton fabric with two different geometries (Figure 20d). Starting with the geometry usually adopted for non-textile OECTs (G1), they developed a new electrode configuration (G2) that operates with few microliters of electrolyte solution, in order to obtain a device able to work with natural

human perspiration. These textile OECTs can be deformed without any degradation of its electrical performance, and their stability is maintained under repetitive hand-washing cycles. The performance of these OECTs for monitoring redox active biomolecules like **adrenaline and dopamine** neurotransmitters, was found to be very close to that of conventional non-textiles OECTs. The working principle of these textile OECTs is based on the electrocatalytic properties of PEDOT:PSS conductive polymer. The PEDOT:PSS channel exhibits a potential which is high enough to electro-oxidize these biomolecules. The oxidation of the analytes gives electrons to PEDOT:PSS, which leads to hole extraction from the transistor channel and subsequent decrease of the channel conductivity. Additionally, the response to adrenaline and dopamine neurotransmitters was also successfully measured in artificial sweat, thus demonstrating that these textile sensors can be potentially used for the detection of biomarkers in external body fluids.

E. Amino Acid Sensing

Recently, Battista *et al.* [95] have expanded the sensing ability of cotton-based OECTs to enzyme-catalyzed reactions without the use of electron mediators. They developed an OECT sensor based on a PEDOT:PSS-modified cotton fiber functionalized with the phenol oxidase enzyme laccase. An advantage of this enzyme relies on the possibility to have a mediatorless catalyzed reaction, increasing the sensitivity of the device. The biosensor is completely wearable and textile-based and was used for direct detection of **L-Tyrosine** (L-Tyr), a natural amino acid, which is a precursor in the biosynthesis of neurotransmitters and hormones, among others. Hyper- and hypothyroidism, hypochondria, dementia or Parkinson can be promoted by the unbalanced concentration of L-Tyr. L-Tyr in aqueous solutions with varying concentrations is detected by the modulation of the signal response and the kinetic of the signal. Modulation of the laccase-functionalized biosensor was found to be proportional to the L-Tyr concentration. The biosensor device can selectively detect this amino acid with good sensitivity, high resolution and repeatability, with a limit of detection of 10^{-8} M. This sensitivity allows the detection of L-Tyr in real human physiological fluids. The kinetics analysis reveals that there is an optimal value of the V_{GS} voltage (0.4-0.6 V) for which the sensor system responds more promptly to the input. Finally, it was demonstrated that adsorption of the enzyme onto the textile surface improves the sensing, both in modulation and response time, probably due to a close interaction of the enzyme (strongly entrapped into the cotton fibers), with the PEDOT:PSS active layer.

F. Glucose Sensing

Many OECT-based glucose biosensors have already been described and although many efforts have been made in improving their performance, most of these devices operate with liquid electrolytes and planar configuration, which is not compatible with miniaturization and wearable devices for portable real-time sensing. Wang *et al.* [96] have developed a woven fiber OECT for glucose sensing (Figure 21a).
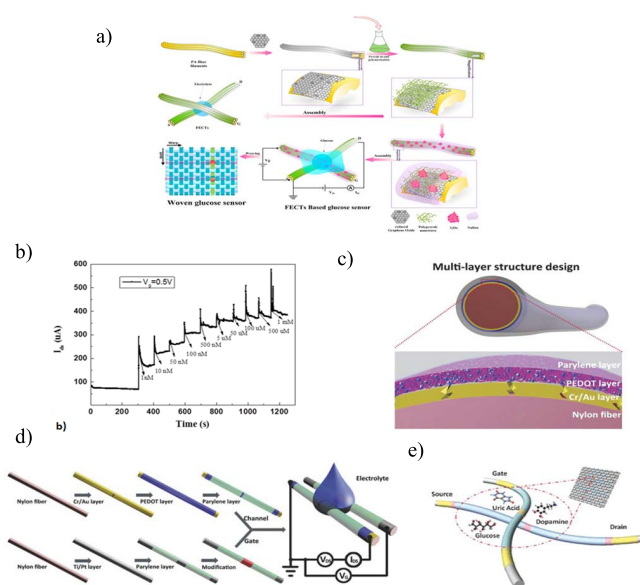

Fig. 21. a) Fabrication of the woven fibre OECT (reproduced from [96] with permission from Elsevier, Copyright © 2017), b) IDS response as a function of time upon addition of glucose at different concentrations (VDS = −2V) (reproduced from [96] with permission from Elsevier, Copyright © 2017), c) Design of a core-shell conductive fibre [97], d) Fabrication process of a fibre-based OECT with functionalized gate [97], e) Design of flexible fabric OECT sensors by weaving fibre-based devices with cotton yarns [97]. (c, d and e were reproduced from [97] with permission from John Wiley and Sons, Copyright © 2018).

The OECT is based on polyamide (PA6) fibers modified with polypyrrole nanowires (PPy) / reduced graphene oxide (rGO) composite as active layer. When glucose is present in the electrolyte, its interaction with GOx modulates the source-drain current (I_{DS}). Contrary to other OECT-based glucose sensors, I_{DS} of this device increases with the increase of glucose concentration, as a consequence of the enzymatic reaction cycle that occurs in the presence of glucose. Glucose is catalyzed by the GOx enzyme at the gate, producing H_2O_2. Usually, the H_2O_2 concentration is directly related to the glucose concentration, and H_2O_2 is often used to detect and measure the glucose content. However, in this woven OECT, H_2O_2 can be reacted sequentially with the strong oxidizing $LiClO_4$ in the electrolyte, allowing electron transfer (faradaic current) near the gate electrode. This decreases the effective gate voltage applied on the OECT, which in turn increases the channel current (Figure 21b). In addition, the device displays good selectivity to glucose in the presence of AA and UA. The higher sensitivity and selectivity to glucose of this woven fiber-based OECT compared to planar configuration OECT-based sensors, is attributed to the three-dimensional structures of fibers with a larger surface-to-volume ratio. The reliability of this glucose fiber sensor was demonstrated in real samples of rabbit blood.

Recently, Yang *et al.* [97] have reported another wearable OECT for detection of glucose. By introducing metal/conductive polymer multilayer electrodes on nylon fibers (Figure 21c), fiber-based OECTs were prepared with very stable performance during bending (Figure 21d). The sensing mechanism of these fiber OECTs when used as

biosensors relies on the electrochemical interaction of the analyte with the gate electrode. Such interaction changes the potential drop at the electric double layer on the gate and leads to the change of the effective gate voltage. These fiber-based OECTs were used as glucose sensors by modifying the Pt gate electrodes with glucose oxidase (GOx) enzyme/chitosan (CHIT)/graphene composite. The channel current of the device decreases with the increase of glucose concentration, with a limit of detection as low as 30×10^{-9} M. Besides the effect of the GOx enzyme on the selectivity, the negatively charged CHIT on the fiber gate electrode serves as an effective blocking layer for interferents such as UA, DA and AA, due to electrostatic forces. Due to their excellent flexibility and bending stability, these fiber-based OECTs can be woven together with cotton yarns using a conventional weaving machine, resulting in flexible stretchable fabric biosensors with high performance (Figure 21e). Due to the capillary effects in fabrics, these sensors show much more stable signals in the analysis of moving aqueous solutions than planar devices. As a potential application, the fabric devices with functionalized gates were successfully used to detect glucose levels of artificial urine. The fabric OECTs were integrated in a diaper and remotely operated with a mobile phone via Bluetooth integrated circuitry. The channel current shows an obvious response when artificial urine was dropped in the diaper, even in the presence of UA interferent, offering a unique platform for wearable healthcare monitoring.

G. Hormone Sensing

Under stress, adrenaline and the hormone cortisol are released in the bloodstream. Increased levels of **cortisol** have a detrimental effect on the regulation of various physiological processes, like blood pressure, glucose levels, and carbohydrate metabolism. Therefore, continuous monitoring of cortisol levels in biofluids can be of great relevance in maintaining healthy physiological conditions. Parlak *et al.* [98] have designed a wearable platform for stress detection by selectively sensing the human hormone cortisol in sweat. The sensing element consists of a molecularly selective OECT (MS-OECT) that integrates an OECT and a taylor-made synthetic and biomimetic polymeric membrane, which acts as a molecular memory layer facilitating the stable and selective recognition of cortisol. The MS-OECT sensor and a laser-patterned microcapillary channel array are integrated in a wearable sweat diagnostics platform. This platform provides accurate sweat acquisition and precise sample delivery to the sensor interface (Figure 22a). The MS-OECT comprises a multifunctional layered structure that achieves selective sensing of cortisol from human sweat (Figure 22b). The device consists of a PEDOT:PSS OECT with planar Ag/AgCl gate as an electrochemical transducing layer, functionalized with molecularly selective membrane (MSM) biorecognition, based on molecularly imprinted polymers (MIPs). MIPs are artificial receptors that are increasingly recognized as a versatile tool for the preparation of synthetic polymers containing tailor-made recognition sites, as an alternative to natural systems to overcome the limitations of unstable biorecognition.
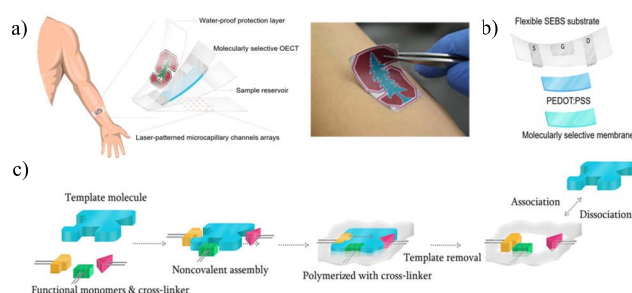

Fig. 22.   a) Patch-type wearable cortisol sensor [98], b) Schematic of the MS-OECT multifunctional layered structure [98], c) Non-covalent imprinting process [98]. Reproduced from [98] with permission from John Wiley and Sons, Copyright © 2018).

Artificial recognition is here achieved by non-covalent imprinting process (Figure 22c).

The MIP-based artificial recognition membrane is interposed between the electrolyte (sweat) reservoir and the PEDOT:PSS channel in order to regulate the selective molecular transport of the analyte (cortisol) directly from the skin to the OECT sensing channel. The working principle of the functionalization of the OECT with molecular recognition is as follows: in the presence of the analyte, the membrane pores are sealed and block ion motion to the channel, strongly reducing the measured change in the source-drain current of the channel, thereby giving rise to a sensing event. These sensing platforms were successfully used with skin-like microfluidics in ex-situ methods. They were further implemented on human subjects with on-body, real-sample analysis using a wearable sensor assembly. Both systems exhibit a log-linear response to cortisol concentrations in the range 0.01-10 μM with sensitivity of 2.68 μA/decade and high selectivity against cortisol structural analogs that are found in sweat and could interfere (like progesterone, cortisone, and testosterone). Hence, these systems display good sensing characteristics in the range of physiological cortisol concentration (0.1-1.0 μM). This multifunctional layered device can be adapted to other sweat-based wearable sensors.

X. REMAINING CHALLENGES IN OECT-BASED BIOSENSORS

OECT-based biosensors have attracted a significant attention in the last decade. Their impressive transconductance, the low operating voltages, their flexibility and ability to transduce ionic signals to electrical signals combined with their low cost (<$10), together with their compatibility with low cost electronics, have given OECTs an immense potential to be used, not only for research purposes, as commercial products in the near future. However, since their discovery in the previous decade, they have yet to reach the required level for commercial products.

OECT-based ion sensors reported sensitivities close to the Nernstian response, which can also be achieved with other available sensors [21], but exceptional OECTs due to their high transconductance showed sensitivities of up to 600 mV/decade concentration of measurant. On the other hand, the reported LODs have a long way to go when compared to sensors involving nanotechnologies and Carbon NanoTubes (CNT) [99]. The reported LODs for OECT-based

ion sensing are in the micromolar range whilst nanotechnology sensors can reach down to the picomolar range. OECTs have also been applied in organic bioelectronics to monitor various types of biological analytes concentration. The achieved sensitivities are up to several μA/decade and with LODs down to the nanomolar scale. Other technologies used for biomolecule detection have achieved better performances hence, more work is required to reach the nanotechnologies levels but these sensors are good enough for use in biological samples since they fall within the required ranges [99]. On the other hand, sensors based on nanotechnologies are several orders of magnitude more expensive. OECT-based sensors for bacterial detection have reached LODs down to 100 cells/ml whilst virus sensors have shown, compared to other sensor technologies, very promising performances with LOD down to 0.025 HemAagglutination Units [100]. Cell-based biosensors have also reported to monitor physiological changes in cells exposed to pathogens, pollutants, biomolecules or drugs. OECTs have been successfully used as cell biosensors to monitor cells-substrate attachment, cells confluence and barrier tissue integrity, transepithelial ion transport, cell stress and death, and cell surface biomolecules. The reported OECTs cell-based sensors have shown impressive temporal resolutions of down to 30 seconds for barrier tissue disruption compared to almost an hour from other reported sensors. Furthermore, OECTs have been used for biomarker detection. Although these devices have opened the doors for implantable devices, they fall behind in performance metrics like LODs, linear range, sensitivity and selectivity compared to other sensors. Reported LODs are in the range of several femtomolar and have linear ranges of up to 7 orders of magnitude. Other sensors based on silicon nanowires for example, have shown LODs down to the attomolar range with similar linear ranges [101], [102]. Nevertheless, silicon nanowire sensors operate at higher voltages and with more complicated electronic readout circuits compared to OECTs.

Additionally, OECTs can achieve a response time well below a millisecond therefore, they make powerful amplifying transducers in biological applications, including recordings of brain and heart activity and electrochemical detection of neurotransmitters. This is probably the most promising sensing application of OECTs. They have exceeded the performances of other electrophysiological sensors with SNR values of up to 52 dB [103]. It is predicted that OECT-based electrophysiological sensors together with possibly wearable and textile sensors, will grow much faster and form a major part of the industry in the coming years.

XI. SUMMARY OF OECT-BASED BIOSENSORS

A comprehensive review of the most important advancements in the field of OECT-based biosensors has been explored in detail. The performances of the different biosensors under consideration here are summarized in Table II.

XII. TRENDS IN OECT FABRICATION

A. Fabrication Technologies

Several fabrication technologies have been used over the years in the early 2000s for OECTs [22], [109]–[115] and,
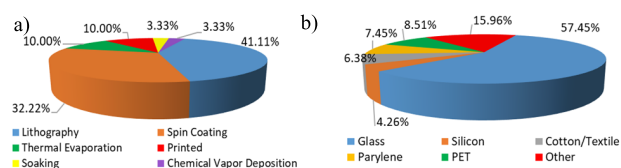

Fig. 23. a) Fabrication technologies and b) substrate materials in OECT-based biosensors.
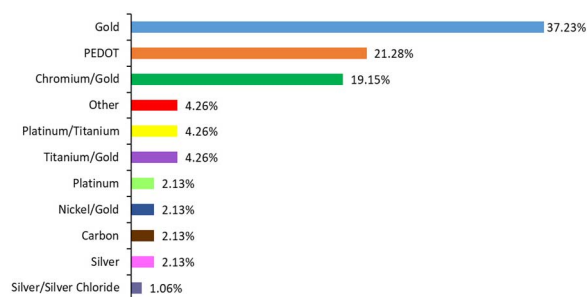

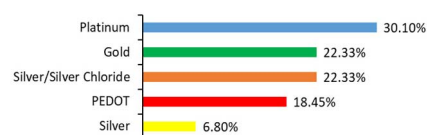Fig. 24. Materials used for source/drain electrodes in OECT-based biosensors.

Fig. 25. Materials used for the gate electrodes in OECT-based biosensors.

more specifically, for OECTs used as biosensors. Although some technologies, such as photolithography and Chemical Vapor Deposition (CVD), offer much better accuracy and repeatability they are usually expensive and might not be compatible with all the electrode and/or substrate materials. In order to overcome these tradeoffs, researchers have combined multiple fabrication technologies, significantly improving the performance of the OECT-based sensors. The statistical results presented in the following figures (Figure 23, Figure 24, Figure 25) were computed by identifying the fabrication technologies reported in each reference reported in this review only. Figure 23a shows an approximation of the technologies used for OECT-based biosensors with lithography being the one used the most. **Lithography** is a very well-known technology that features impressive resolutions, accuracy and repeatability [109], [111], [112], [114]. However, it has limitations related to its very high costs, and in terms of the materials used. Hence, spin coating, thermal evaporation or CVD are usually combined with lithography to overcome those restrictions.

Additionally, **printing technologies** (like thick-film technology and inkjet printing) [110], [113], [115] are now emerging as suitable fabrication technologies for sensing purposes. These technologies are able to overcome the expensive fabrication procedures of lithography, although being less accurate and reliable. Printing technologies feature another very important advantage: they are compatible with

TABLE II
SUMMARY OF OECT-BASED BIOSENSORS

	Analyte/Target	Performance	Reference
Ion sensors	H^+, K^+, Na^+, Ca^{2+}, Al^{3+}	Sensitivities: 64.2 mV/decade (H^+) 59.4 mV/decade (K^+) 57.7 mV/decade (Na^+) 29.7 mV/decade (Ca^{2+}) 17.6 mV/decade (Al^{3+})	[23]
Ion sensors	K^+	Linear response: 10^{-4} M - 10^{-1} M Sensitivity: 48 mV/decade LOD = 1.5×10^{-5} M	[24]
Ion sensors	K^+, Na^+	Sensitivities: 414 mV/decade (K^+) 516 mV/decade (Na^+)	[25]
Ion sensors	K^+, Na^+, Ca^{2+}	g_m = 43 mS LOD = 1 mM Linear response: 1 - 10 mM Sensitivities: 650 mV/decade (Na^+) 516 mV/decade (Ca^{2+}) 366 mV/decade (K^+)	[26]
Ion sensors	Na^+	Sensitivity: 146 mV/decade LOD = 10^{-6} M	[27]
Ion sensors	pH	pH range: 5 - 7.3	[28]
Ion sensors	pH	Sensitivity: 93 ± 8 mV/pH	[29]
Biomolecules/enzymes sensors	Glucose	LOD = 10^{-4} M	[32]
Biomolecules/enzymes sensors	Glucose	LOD = 10^{-6} M	[104], [105]
Biomolecules/enzymes sensors	Glucose	LOD = 10^{-7} M	[35]
Biomolecules/enzymes sensors	Glucose	Sensitivity: 0.01 NR / 1 μM	[33]
Biomolecules/enzymes sensors	Glucose	LOD = 5×10^{-9} M	[36]
Biomolecules/enzymes sensors	Glucose	LOD = 30×10^{-9} M	[38]
Biomolecules/enzymes sensors	Dopamine	LOD = 5×10^{-9} M	[41]
Biomolecules/enzymes sensors	Dopamine	Sensitivity: 9.1 S $M^{-1}cm^{-2}$ LOD = 6×10^{-6} M	[106]
Biomolecules/enzymes sensors	Dopamine	Response time: 10^{-5} s Linear response: 10^{-7} M - 10^{-5} M Sensitivity: 45.2 mV/decade LOD = 1 nM	[107]
Biomolecules/enzymes sensors	Dopamine	LOD = 37 nM Linear response: 50 nM -100 μM	[108]
Biomolecules/enzymes sensors	Epinephrine	LOD = 0.1 nM	[42]
Biomolecules/enzymes sensors	Epinephrine	LOD = 90 pM Linear response: 90 pM - 900 nM	[43]
Biomolecules/enzymes sensors	Glutamate/Acetylcoline	LOD = 5 μM Sensitivities: 4.3 A mol^{-1} L cm^{-2} (Glutamate) 4.1 A mol^{-1} L cm^{-2} (ACh)	[44]
Biomolecules/enzymes sensors	Lecithin Lecithin-chitosan	LOD = 10^{-4} mg/ml (L) LOD = 10^{-5} mg/ml (LC)	[45]
Biomolecules/enzymes sensors	Eumelanin	LOD = 10^{-6} M	[46]
Biomolecules/enzymes sensors	Gallic acid	LOD = 10 nM	[47]
Biomolecules/enzymes sensors	Ascorbic acid	Linear response: 10^{-6} M - 10^{-3} M Sensitivity: 4.5×10^{-6} A/decade LOD = 13 nM	[48]
Biomolecules/enzymes sensors	Ascorbic acid	Linear response: 1 μM -100 μM Sensitivity: 75.3 μA/decade LOD = 10 nM	[49]
Biomolecules/enzymes sensors	D/L-Histidine	Linear response: 100 nM - 10 μM LOD = 10 nM (D-His) LOD = 100 nM (L-His)	[51]
Biomolecules/enzymes sensors	L-Tryptophan	Linear response: 300 nM - 10 μM Sensitivity: 3.19 μA/μM LOD = 2 nM	[50]

TABLE II
(Continued.) SUMMARY OF OECT-BASED BIOSENSORS

Biomolecules/enzymes sensors	L-Tyrosine	Linear response: 300 nM - 10 µM Sensitivity: 3.64 µA/µM LOD = 30 nM	[50]
Biomolecules/enzymes sensors	Sialic acid	LOD = 8 mM (free SA) LOD = 4×10^3 cells/ml (HeLa cells)	[52]
Biomolecules/enzymes sensors	Sarcosine	Linear response: 50 nM - 100 µM Sensitivity: 58.6 mV/decade LOD = 50 nM	[53]
Biomolecules/enzymes sensors	Glucose and lactate	LOD = 10^{-7} M (glucose) LOD = 10^{-6} M (lactate)	[54]
Biomolecules/enzymes sensors	Glucose, lactate and cholesterol	-	[55]
Bacteria/virus sensors	Escherichia coli	LOD = 10^{-3} cfu/ml	[56]
Bacteria/virus sensors	Navicula sp Amphiprore sp	LOD = 100 cell/ml (Navicula) LOD = 400 cell/ml (Amphiprore)	[57]
Bacteria/virus sensors	Human Influenza A	LOD = 0.025 HAU	[60]
Cell-based sensors	Ion transport	g_m = 2000 µS Response time constant: 100 µs Sensitivity: 54.7 mV/decade	[70]
Cell-based sensors	Cell death	Detection limit: 0.5 µM	[71]
Cell-based sensors	Cell surface biomolecules	Detection limit: 10 cells/µl	[72]
Immunosensors	Prostate Specific Antigen	LOD = 1 pg/ml Sensitivity: 0.0976 mA (pg/ml)$^{-1}$	[73]
Immunosensors	Human Epidermal growth factor Receptor 2	Linear response: 10^{-7} - 10^{-14} g/ml LOD = 10^{-14} g/ml	[74]
Immunosensors	Interleukin-6	LOD = 220 pg/ml	[75]
Nucleotide sensors	cDNA	LOD = 10 pM	[76]
Nucleotide sensors	cDNA	LOD = 0.1 nM	[77]
Nucleotide sensors	microRNA21	Linear response: 5 pM - 20 nM LOD = 2 pM	[79]
Electrophysiological sensors	Brain activity	SNR = 52.7 dB	[80]
Electrophysiological sensors	Heart activity	Detection limit: µV_{SG} = 50 µV Time constant: 1.5 ms	[82]
Electrophysiological sensors	Heart activity	g_m = 2.5 mS propagation velocity: 100 µm/ms action potential duration: 10.3 ms action potential rise time: 0.46 ms	[83]
Electrophysiological sensors	Heart activity	g_m = 12 mS	[84]
Electrophysiological sensors	Heart activity	g_m = 1 mS SNR = 52 dB	[85]
Wearable sensors	Na$^+$	Response time: 30s LOD = 17.1 µM	[87]
Wearable sensors	Pb^{2+}	Linear response: 10^{-5} - 10^{-2} M Sensitivity: 446 µA/decade LOD = 10^{-5} M on/off ratio: 10^4	[88]
Wearable sensors	Ethanol	LOD = 0.0004 wt% BAC = 0.01% - 0.2%	[89]
Wearable sensors	Lactate	Linear response: 10 -100 mM	[90]
Wearable sensors	Lactate	Sensitivity: 1.9 mA/mM	[91]
Wearable sensors	Adrenaline	LOD = 10^{-6} M	[92]
Wearable sensors	Dopamine	Response time: 0.5 s Sensitivity: 47.28 NCR/decade	[93]
Wearable sensors	Dopamine	Linear response: 2×10^{-6}- 3×10^{-5} M Sensitivity: 10^{-6} M	[94]
Wearable sensors	Adrenaline	Linear response: 3×10^{-5}- 5×10^{-4} M Sensitivity: 0.75×10^{-5} M	[94]
Wearable sensors	L-Tyrosine	LOD = 10^{-8} M Response time: 40 min	[95]
Wearable sensors	Glucose	Linear response: 1 nM - 5 µM Sensitivity: 0.773 NCR/decade Response time: 0.5 s On/off ratio: 10^2	[96]
Wearable sensors	Glucose	LOD = 30×10^{-9} M	[97]
Wearable sensors	Cortisol	Linear response: 0.01 - 10 µM Sensitivity: 2.68 mA/decade	[98]

a much wider variety of substrates and with a much broader range of electrode materials (gate, source, drain electrodes). The use of printing technologies is preferred therefore for sensing applications, whilst lithographic fabrication is more widely used for the fabrication of precise and smaller electronic components.

Figure 23b shows an approximation of the distribution of the different **substrate materials** used for OECT-based biosensors. It has to be noted that glass and silicon substrates are usually used when the OECTs are fabricated with lithography making them rigid devices, whereas in the case of flexible substrates (such as textiles, PET and parylene), printing, coating and soaking technologies are preferred.

B. Electrodes and Semiconducting Materials

Although the general geometry of the OECT can greatly affect the performance of the device, the materials used as source/drain electrodes also play an important role. Depending on whether the functionalization happens on the semiconducting material itself or on one of the electrodes, different materials have been used by researchers to accommodate for their specific application. On the other hand, if the purpose of the OECT-based biosensor is to have an all-organic device that can be fully biocompatible (especially in the case of implantable sensors), then it is required to use an organic material for the gate, source and drain electrodes.

The **semiconducting polymer** used in an OECT is probably more important than the electrode material. The conducting polymer can be either p-type or n-type and depending on the kind of charges to be detected, the appropriate type must be used. The performance of the OECT-based biosensor is strongly dependent on the polymer, because it determines the ion-to-electron conversion ratio. In reality, more than 90% of the reported OECT-based biosensors use PEDOT:PSS due to its ease of use, compatibility with multiple technologies, high transconductance compared to other organic semiconductors, and its stability and repeatability during fabrication. Furthermore, PEDOT:PSS can be easily functionalized in a wide temperature range and it is biocompatible hence, its wide use in biomedical sensing.

Concerning the **source/drain electrodes**, Figure 24 shows the percentages of the materials used for these electrodes in OECT-based biosensors. Gold is the most commonly used material because of its compatibility with almost all fabrication technologies, high conductivity, low tendency to react with other species and very easy functionalization. Up to 60% of the reported sensors use pure gold or a gold mixture for the source/drain electrodes.

The second most used material is PEDOT:PSS, making the device much simpler, lower cost and compatible with more technologies.

Figure 25 shows the percentages of materials used for the **gate electrode**. Platinum is the most commonly used material for gate electrodes due to its stability, high conductivity and easy functionalization. In this case, PEDOT:PSS is not so widely used. Unless the application requires an all-organic device, metal gate electrodes (Au, Pt) are preferred due to their much easier functionalization.

XIII. Conclusion

OECTs have become an important emerging platform for flexible, biocompatible biosensors due to their flexibility, low cost, biocompatibility and most importantly their incomparable transconductance in terms of ion-to-electron conversion. Initially, the device physics based on the Bernard model has been explored together with a brief comparison with conventional MOSFET transistors.

A comprehensive review of OECT-based biosensors has been provided highlighting the most important challenges and obstacles that appeared during their evolution. Biologically important ions such as hydrogen, potassium, sodium and calcium, have been detected using OECTs with sensitivities of up to 650 mV/ decade of ion concentration. These sensitivities are significantly better than any other transistor- based ion sensor. However, the LODs reported are comparable to other sensing techniques. Biomolecule and enzyme-based biosensors have been described showing remarkable sensitivities and LODs. Their most intriguing feature is that they can be used with untreated samples and in-situ, due to the biocompatibility of their building materials. Biomolecules such as glucose, dopamine, epinephrine, ascorbic acid, eumelanin and lactic acid have been detected using OECTs showing sensitivities of 2-5 μA/μM and LODs in the range of several nM. Other than detecting important biomolecules, OECTs have been successfully used to detect bacteria and viruses, such as E. coli and Human Influenza A, whilst they were also used to detect cell morphology and death. Later, OECT-based immunosensors have been explored showing the ability to detect PSA, and Interleukin-6. Some more recent works have reported the detection of complimentary DNA and miRNA with impressive sensitivities and LODs down to 2 pM.

Other than the remarkable ability of OECTs to act like ion-to-electron converters with very high transconductances, these devices were also used as electrophysiological sensors to monitor the electrical activity of the brain and heart. Outstanding signal-to-noise ratios have been reported up to 52.7 dB with transconductances of more than 10 mS.

One of the most common approaches using OECT-based biosensors are wearable sensors. These devices offer high flexibilities, which is a very important factor for wearables, but they further allow their construction using woven fibres. This kind of woven fibre-based OECTs have been used to monitor glucose, cortisol, adrenaline and dopamine levels on human subjects with unmatched performances. These structures are very promising in the area of textile electronics with the potential to monitor human health markers through clothes, with the ability to connect them to the Internet of Things in the future.

Finally, a statistical analysis of the trend in the field has been given in terms of fabrication technologies, source/drain and gate electrodes as well as organic semiconducting materials. The most important tradeoffs between fabrication technologies have been highlighted, which can explain the reasons why materials like PEDOT:PSS and gold-based electrodes are mostly chosen for semiconducting and source/drain electrodes, respectively. It is believed that printing technologies will be the major fabrication technologies for OECT-based biosensors

because they are low cost, allowing for disposable sensing platforms, but also because they show a much wider versatility in terms of substrates and printing materials.

REFERENCES

[1] M. Riordan. (2020). *Transistor–Electronics Encyclopaedia Brittanica*. [Online]. Available: https://www.britannica.com/technology/transistor/Junction-transistors

[2] S. Datta, "Recent advances in high performance CMOS transistors: From planar to non-planar," *Interface Mag.*, vol. 22, no. 1, pp. 41–46, Jan. 2013, doi: 10.1149/2.F04131if.

[3] M. Berggren and A. Richter-Dahlfors, "Organic bioelectronics," *Adv. Mater.*, vol. 19, no. 20, pp. 3201–3213, 2007, doi: 10.1002/adma.200700419.

[4] J. T. Mabeck and G. G. Malliaras, "Chemical and biological sensors based on organic thin-film transistors," *Anal. Bioanal. Chem.*, vol. 384, no. 2, pp. 343–353, Dec. 2005, doi: 10.1007/s00216-005-3390-2.

[5] X. Strakosas, M. Bongo, and R. M. Owens, "The organic electrochemical transistor for biological applications," *J. Appl. Polym. Sci.*, vol. 132, no. 15, pp. 1–14, 2015, doi: 10.1002/app.41735.

[6] E. Garcia-Breijo, B. Gomez-Lor Perez, and P. Cosseddu, *Organic Sensors Materials and Applications*. 2016, doi: 10.1007/978-94-017-9780-1_6.

[7] M. Ates, "A review study of (bio)sensor systems based on conducting polymers," *Mater. Sci. Eng., C*, vol. 33, no. 4, pp. 1853–1859, May 2013, doi: 10.1016/j.msec.2013.01.035.

[8] J. Rivnay, S. Inal, A. Salleo, R. M. Owens, M. Berggren, and G. G. Malliaras, "Organic electrochemical transistors," *Nature Rev. Mater.*, vol. 3, no. 2, p. 17086, Feb. 2018, doi: 10.1038/natrevmats.2017.86.

[9] D. A. Bernards and G. G. Malliaras, "Steady-state and transient behavior of organic electrochemical transistors," *Adv. Funct. Mater.*, vol. 17, no. 17, pp. 3538–3544, Nov. 2007, doi: 10.1002/adfm.200601239.

[10] D. Wang, V. Noël, and B. Piro, "Electrolytic gated organic field-effect transistors for application in biosensors—A Review," *Electronics*, vol. 5, no. 1, p. 9, 2016. [Online]. Available: https://doi.org/10.3390/electronics5010009.

[11] J. T. Friedlein, R. R. McLeod, and J. Rivnay, "Device physics of organic electrochemical transistors," *Organic Electron.*, vol. 63, pp. 398–414, Dec. 2018, doi: 10.1016/j.orgel.2018.09.010.

[12] B. Piro *et al.*, "Fabrication and use of organic electrochemical transistors for sensing of metabolites in aqueous media," *Appl. Sci.*, vol. 8, no. 6, p. 928, Jun. 2018, doi: 10.3390/app8060928.

[13] A.-M. Pappa, O. Parlak, G. Scheiblin, P. Mailley, A. Salleo, and R. M. Owens, "Organic electronics for point-of-care metabolite monitoring," *Trends Biotechnol.*, vol. 36, no. 1, pp. 45–59, Jan. 2018, doi: 10.1016/j.tibtech.2017.10.022.

[14] L. Kergoat, B. Piro, M. Berggren, G. Horowitz, and M.-C. Pham, "Advances in organic transistor-based biosensors: From organic electrochemical transistors to electrolyte-gated organic field-effect transistors," *Anal. Bioanal. Chem.*, vol. 402, no. 5, pp. 1813–1826, Feb. 2012, doi: 10.1007/s00216-011-5363-y.

[15] G. Tarabella *et al.*, "New opportunities for organic electronics and bioelectronics: Ions in action," *Chem. Sci.*, vol. 4, no. 4, pp. 1395–1409, Dec. 2012, doi: 10.1039/c2sc21740f.

[16] J. Liao, H. Si, X. Zhang, and S. Lin, "Functional sensing interfaces of PEDOT:PSS organic electrochemical transistors for chemical and biological sensors: A mini review," *Sensors*, vol. 19, no. 2, p. 218, Jan. 2019, doi: 10.3390/s19020218.

[17] N. Wang, A. Yang, Y. Fu, Y. Li, and F. Yan, "Functionalized organic thin film transistors for biosensing," *Accounts Chem. Res.*, vol. 52, no. 2, pp. 277–287, Feb. 2019, doi: 10.1021/acs.accounts.8b00448.

[18] L. Bai, C. G. Elósegui, W. Li, P. Yu, J. Fei, and L. Mao, "Biological applications of organic electrochemical transistors: Electrochemical biosensors and electrophysiology recording," *Frontiers Chem.*, vol. 7, pp. 1–16, May 2019, doi: 10.3389/fchem.2019.00313.

[19] Electrical4U. (2018). *MOSFET Characteristics*. Accessed: Apr. 5, 2020. [Online]. Available: https://www.electrical4u.com/mosfet-characteristics/

[20] D. Khodagholy *et al.*, "High transconductance organic electrochemical transistors," *Nature Commun.*, vol. 4, no. 1, pp. 1–6, Oct. 2013, doi: 10.1038/ncomms3133.

[21] J. Bobacka, A. Ivaska, and A. Lewenstam, "Potentiometric ion sensors," *Chem. Rev.*, vol. 108, no. 2, pp. 329–351, Feb. 2008, doi: 10.1021/cr068100w.

[22] D. A. Bernards, G. G. Malliaras, G. E. S. Toombes, and S. M. Gruner, "Gating of an organic transistor through a bilayer lipid membrane with ion channels," *Appl. Phys. Lett.*, vol. 89, no. 5, pp. 87–90, 2006, doi: 10.1063/1.2266250.

[23] P. Lin, F. Yan, and H. L. W. Chan, "Ion-sensitive properties of organic electrochemical transistors," *ACS Appl. Mater. Interfaces*, vol. 2, no. 6, pp. 1637–1641, Jun. 2010, doi: 10.1021/am100154e.

[24] M. Sessolo, J. Rivnay, E. Bandiello, G. G. Malliaras, and H. J. Bolink, "Ion-selective organic electrochemical transistors," *Adv. Mater.*, vol. 26, no. 28, pp. 4803–4807, Jul. 2014, doi: 10.1002/adma.201400731.

[25] M. Ghittorelli *et al.*, "High-sensitivity ion detection at low voltages with current-driven organic electrochemical transistors," *Nature Commun.*, vol. 9, no. 1, pp. 1–10, Dec. 2018, doi: 10.1038/s41467-018-03932-3.

[26] D. Majak, J. Fan, and M. Gupta, "Fully 3D printed OECT based logic gate for detection of cation type and concentration," *Sens. Actuators B, Chem.*, vol. 286, pp. 111–118, May 2019, doi: 10.1016/j.snb.2019.01.120.

[27] X. Wu *et al.*, "Ionic-liquid doping enables high transconductance, fast response time, and high ion sensitivity in organic electrochemical transistors," *Adv. Mater.*, vol. 31, no. 2, 2019, Art. no. 1805544, doi: 10.1002/adma.201805544.

[28] G. Scheiblin, R. Coppard, R. M. Owens, P. Mailley, and G. G. Malliaras, "Referenceless pH sensor using organic electrochemical transistors," *Adv. Mater. Technol.*, vol. 2, no. 2, Feb. 2017, Art. no. 1600141, doi: 10.1002/admt.201600141.

[29] F. Mariani, I. Gualandi, M. Tessarolo, B. Fraboni, and E. Scavetta, "PEDOT: dye-based, flexible organic electrochemical transistor for highly sensitive pH monitoring," *ACS Appl. Mater. Interfaces*, vol. 10, no. 26, pp. 22474–22484, Jul. 2018, doi: 10.1021/acsami.8b04970.

[30] D. J. Macaya, M. Nikolou, S. Takamatsu, J. T. Mabeck, R. M. Owens, and G. G. Malliaras, "Simple glucose sensors with micromolar sensitivity based on organic electrochemical transistors," *Sens. Actuators B, Chem.*, vol. 123, no. 1, pp. 374–378, Apr. 2007, doi: 10.1016/j.snb.2006.08.038.

[31] P. N. Bartlett, "Measurement of low glucose concentrations using a microelectrochemical enzyme transistor," *Analyst*, vol. 123, no. 2, pp. 387–392, 1998, doi: 10.1039/a706296f.

[32] Z.-T. Zhu, J. T. Mabeck, C. Zhu, N. C. Cady, C. A. Batt, and G. G. Malliaras, "A simple poly (3, 4-ethylene dioxythiophene)/poly (styrene sulfonic acid) transistor for glucose sensing at neutral pH," *Chem. Commun.*, pp. 1556–1557, 2004.

[33] S. K. Kanakamedala, H. T. Alshakhouri, M. Agarwal, and M. A. DeCoster, "A simple polymer based electrochemical transistor for micromolar glucose sensing," *Sens. Actuators B, Chem.*, vol. 157, no. 1, pp. 92–97, Sep. 2011, doi: 10.1016/j.snb.2011.03.030.

[34] N. Y. Shim *et al.*, "All-plastic electrochemical transistor for glucose sensing using a ferrocene mediator," *Sensors*, vol. 9, no. 12, pp. 9896–9902, Dec. 2009, doi: 10.3390/s91209896.

[35] S. Y. Yang *et al.*, "Electrochemical transistors with ionic liquids for enzymatic sensing," *Chem. Commun.*, vol. 46, no. 42, p. 7972, 2010, doi: 10.1039/c0cc02064h.

[36] H. Tang, F. Yan, P. Lin, J. Xu, and H. L. W. Chan, "Highly sensitive glucose biosensors based on organic electrochemical transistors using platinum gate electrodes modified with enzyme and nanomaterials," *Adv. Funct. Mater.*, vol. 21, no. 12, pp. 2264–2272, Jun. 2011, doi: 10.1002/adfm.201002117.

[37] C. Liao, M. Zhang, L. Niu, Z. Zheng, and F. Yan, "Highly selective and sensitive glucose sensors based on organic electrochemical transistors with graphene-modified gate electrodes," *J. Mater. Chem. B*, vol. 1, no. 31, pp. 3820–3829, 2013, doi: 10.1039/c3tb20451k.

[38] C. Liao, C. Mak, M. Zhang, H. L. W. Chan, and F. Yan, "Flexible organic electrochemical transistors for highly selective enzyme biosensors and used for saliva testing," *Adv. Mater.*, vol. 27, no. 4, pp. 676–681, Jan. 2015, doi: 10.1002/adma.201404378.

[39] J. Liao, S. Lin, Y. Yang, K. Liu, and W. Du, "Highly selective and sensitive glucose sensors based on organic electrochemical transistors using TiO₂ nanotube arrays-based gate electrodes," *Sens. Actuators B, Chem.*, vol. 208, pp. 457–463, Mar. 2015, doi: 10.1016/j.snb.2014.11.038.

[40] M. E. Welch, T. Doublet, C. Bernard, G. G. Malliaras, and C. K. Ober, "A glucose sensor via stable immobilization of the GOx enzyme on an organic transistor using a polymer brush," *J. Polym. Sci. A: Polym. Chem.*, vol. 53, no. 2, pp. 372–377, Jan. 2015, doi: 10.1002/pola.27392.

[41] H. Tang, P. Lin, H. L. W. Chan, and F. Yan, "Highly sensitive dopamine biosensors based on organic electrochemical transistors," *Biosensors Bioelectron.*, vol. 26, no. 11, pp. 4559–4563, Jul. 2011, doi: 10.1016/j.bios.2011.05.025.

[42] C. H. Mak *et al.*, "Highly-sensitive epinephrine sensors based on organic electrochemical transistors with carbon nanomaterial modified gate electrodes," *J. Mater. Chem. C*, vol. 3, no. 25, pp. 6532–6538, 2015, doi: 10.1039/c5tc01100k.

[43] N. Saraf, E. R. Woods, M. Peppler, and S. Seal, "Highly selective aptamer based organic electrochemical biosensor with pico-level detection," *Biosensors Bioelectron.*, vol. 117, pp. 40–46, Oct. 2018, doi: 10.1016/j.bios.2018.05.031.

[44] L. Kergoat, B. Piro, D. T. Simon, M.-C. Pham, V. Noël, and M. Berggren, "Detection of glutamate and acetylcholine with organic electrochemical transistors based on conducting polymer/platinum nanoparticle composites," *Adv. Mater.*, vol. 26, no. 32, pp. 5658–5664, Aug. 2014, doi: 10.1002/adma.201401608.

[45] G. Tarabella *et al.*, "Liposome sensing and monitoring by organic electrochemical transistors integrated in microfluidics," *Biochimica et Biophysica Acta (BBA)-Gen. Subjects*, vol. 1830, no. 9, pp. 4374–4380, Sep. 2013, doi: 10.1016/j.bbagen.2012.12.018.

[46] G. Tarabella *et al.*, "Irreversible evolution of eumelanin redox states detected by an organic electrochemical transistor: En route to bioelectronics and biosensing," *J. Mater. Chem. B*, vol. 1, no. 31, p. 3843, 2013, doi: 10.1039/c3tb20639d.

[47] C. Xiong *et al.*, "Highly sensitive detection of gallic acid based on organic electrochemical transistors with poly(diallyldimethylammonium chloride) and carbon nanomaterials nanocomposites functionalized gate electrodes," *Sens. Actuators B, Chem.*, vol. 246, pp. 235–242, Jul. 2017, doi: 10.1016/j.snb.2017.02.025.

[48] I. Gualandi, M. Marzocchi, E. Scavetta, M. Calienni, A. Bonfiglio, and B. Fraboni, "A simple all-PEDOT:PSS electrochemical transistor for ascorbic acid sensing," *J. Mater. Chem. B*, vol. 3, no. 33, pp. 6753–6762, 2015, doi: 10.1039/c5tb00916b.

[49] L. Zhang *et al.*, "Highly selective and sensitive sensor based on an organic electrochemical transistor for the detection of ascorbic acid," *Biosensors Bioelectron.*, vol. 100, pp. 235–241, Feb. 2018, doi: 10.1016/j.bios.2017.09.006.

[50] L. Zhang *et al.*, "Chirality detection of amino acid enantiomers by organic electrochemical transistor," *Biosensors Bioelectron.*, vol. 105, pp. 121–128, May 2018, doi: 10.1016/j.bios.2018.01.035.

[51] L. Zhang *et al.*, "Selective recognition of histidine enantiomers using novel molecularly imprinted organic transistor sensor," *Organic Electron.*, vol. 61, pp. 254–260, Oct. 2018, doi: 10.1016/j.orgel.2018.05.063.

[52] X. Guo *et al.*, "Label-free and sensitive sialic acid biosensor based on organic electrochemical transistors," *Sens. Actuators B, Chem.*, vol. 240, pp. 1075–1082, Mar. 2017, doi: 10.1016/j.snb.2016.09.099.

[53] J. Hu, W. Wei, S. Ke, X. Zeng, and P. Lin, "A novel and sensitive sarcosine biosensor based on organic electrochemical transistor," *Electrochim. Acta*, vol. 307, pp. 100–106, Jun. 2019, doi: 10.1016/j.electacta.2019.03.180.

[54] X. Ji *et al.*, "Highly sensitive metabolite biosensor based on organic electrochemical transistor integrated with microfluidic channel and poly(N-vinyl-2-pyrrolidone)-capped platinum nanoparticles," *Adv. Mater. Technol.*, vol. 1, no. 5, Aug. 2016, Art. no. 1600042, doi: 10.1002/admt.201600042.

[55] A.-M. Pappa *et al.*, "Organic transistor arrays integrated with finger-powered microfluidics for multianalyte saliva testing," *Adv. Healthcare Mater.*, vol. 5, no. 17, pp. 2295–2302, Sep. 2016, doi: 10.1002/adhm.201600494.

[56] R.-X. He *et al.*, "Detection of bacteria with organic electrochemical transistors," *J. Mater. Chem.*, vol. 22, no. 41, pp. 22072–22076, 2012, doi: 10.1039/c2jm33667g.

[57] J. Liao *et al.*, "Organic electrochemical transistor based biosensor for detecting marine diatoms in seawater medium," *Sens. Actuators B, Chem.*, vol. 203, pp. 677–682, Nov. 2014, doi: 10.1016/j.snb.2014.07.052.

[58] C. Pitsalidis *et al.*, "Biomimetic electronic devices for measuring bacterial membrane disruption," *Adv. Mater.*, vol. 30, no. 39, 2018, Art. no. 1803130, doi: 10.1002/adma.201803130.

[59] S. A. Tria *et al.*, "Dynamic monitoring of salmonella typhimurium infection of polarized epithelia using organic transistors," *Adv. Healthcare Mater.*, vol. 3, no. 7, pp. 1053–1060, 2014. [Online]. Available: https://doi.org/10.1002/adhm.201300632.

[60] W. Hai *et al.*, "Human influenza virus detection using sialyllactose-functionalized organic electrochemical transistors," *Sens. Actuators B, Chem.*, vol. 260, pp. 635–641, May 2018, doi: 10.1016/j.snb.2018.01.081.

[61] P. Lin, F. Yan, J. Yu, H. L. W. Chan, and M. Yang, "The application of organic electrochemical transistors in cell-based biosensors," *Adv. Mater.*, vol. 22, no. 33, pp. 3655–3660, Sep. 2010, doi: 10.1002/adma.201000971.

[62] L. H. Jimison *et al.*, "Measurement of barrier tissue integrity with an organic electrochemical transistor," *Adv. Mater.*, vol. 24, no. 44, pp. 5919–5923, Nov. 2012, doi: 10.1002/adma.201202612.

[63] R. Rao, R. D. Baker, and S. S. Baker, "Inhibition of oxidant-induced barrier disruption and protein tyrosine phosphorylation in Caco-2 cell monolayers by epidermal growth factor," *Biochem. Pharmacol.*, vol. 57, no. 6, pp. 685–695, 1999, doi: 10.1016/S0006-2952(98)00333-5.

[64] S. A. Tria, L. H. Jimison, A. Hama, M. Bongo, and R. M. Owens, "Validation of the organic electrochemical transistor for in vitro toxicology," *Biochimica et Biophysica Acta (BBA)-Gen. Subjects*, vol. 1830, no. 9, pp. 4381–4390, Sep. 2013, doi: 10.1016/j.bbagen.2012.12.003.

[65] M. Ramuz, A. Hama, M. Huerta, J. Rivnay, P. Leleux, and R. M. Owens, "Combined optical and electronic sensing of epithelial cells using planar organic transistors," *Adv. Mater.*, vol. 26, no. 41, pp. 7083–7090, Nov. 2014, doi: 10.1002/adma.201401706.

[66] M. Ramuz *et al.*, "Optimization of a planar all-polymer transistor for characterization of barrier tissue," *ChemPhysChem*, vol. 16, no. 6, pp. 1210–1216, Apr. 2015, doi: 10.1002/cphc.201402878.

[67] M. Ramuz, A. Hama, J. Rivnay, P. Leleux, and R. M. Owens, "Monitoring of cell layer coverage and differentiation with the organic electrochemical transistor," *J. Mater. Chem. B*, vol. 3, no. 29, pp. 5971–5977, 2015, doi: 10.1039/c5tb00922g.

[68] V. F. Curto *et al.*, "Organic transistor platform with integrated microfluidics for in-line multi-parametric in vitro cell monitoring," *Microsyst. Nanoeng.*, vol. 3, no. 1, pp. 1–12, Dec. 2017, doi: 10.1038/micro-nano.2017.28.

[69] S. Y. Yeung, X. Gu, C. M. Tsang, S. W. Tsao, and I.-M. Hsing, "Engineering organic electrochemical transistor (OECT) to be sensitive cell-based biosensor through tuning of channel area," *Sens. Actuators A, Phys.*, vol. 287, pp. 185–193, Mar. 2019, doi: 10.1016/j.sna.2018.12.032.

[70] C. Yao, C. Xie, P. Lin, F. Yan, P. Huang, and I.-M. Hsing, "Organic electrochemical transistor array for recording transepithelial ion transport of human airway epithelial cells," *Adv. Mater.*, vol. 25, no. 45, pp. 6575–6580, Dec. 2013, doi: 10.1002/adma.201302615.

[71] A. Romeo *et al.*, "Drug-induced cellular death dynamics monitored by a highly sensitive organic electrochemical system," *Biosensors Bioelectron.*, vol. 68, pp. 791–797, Jun. 2015, doi: 10.1016/j.bios.2015.01.073.

[72] L. Chen *et al.*, "Organic electrochemical transistors for the detection of cell surface Glycans," *ACS Appl. Mater. Interfaces*, vol. 10, no. 22, pp. 18470–18477, Jun. 2018, doi: 10.1021/acsami.8b01987.

[73] D.-J. Kim, N.-E. Lee, J.-S. Park, I.-J. Park, J.-G. Kim, and H. J. Cho, "Organic electrochemical transistor based immunosensor for prostate specific antigen (PSA) detection using gold nanoparticles for signal amplification," *Biosensors Bioelectron.*, vol. 25, no. 11, pp. 2477–2482, Jul. 2010, doi: 10.1016/j.bios.2010.04.013.

[74] Y. Fu, N. Wang, A. Yang, H. K. wai Law, L. Li, and F. Yan, "Highly sensitive detection of protein biomarkers with organic electrochemical transistors," *Adv. Mater.*, vol. 29, no. 41, pp. 1–7, 2017, Art. no. 1703787, doi: 10.1002/adma.201703787.

[75] D. Gentili *et al.*, "Integration of organic electrochemical transistors and immuno-affinity membranes for label-free detection of interleukin-6 in the physiological concentration range through antibody–antigen recognition," *J. Mater. Chem. B*, vol. 6, no. 33, pp. 5400–5406, 2018, doi: 10.1039/c8tb01697f.

[76] P. Lin, X. Luo, I.-M. Hsing, and F. Yan, "Organic electrochemical transistors integrated in flexible microfluidic systems and used for label-free DNA sensing," *Adv. Mater.*, vol. 23, no. 35, pp. 4035–4040, Sep. 2011, doi: 10.1002/adma.201102017.

[77] W. Tao, P. Lin, J. Hu, S. Ke, J. Song, and X. Zeng, "A sensitive DNA sensor based on an organic electrochemical transistor using a peptide nucleic acid-modified nanoporous gold gate electrode," *RSC Adv.*, vol. 7, no. 82, pp. 52118–52124, 2017, doi: 10.1039/c7ra09832d.

[78] A.-M. Pappa *et al.*, "Polyelectrolyte layer-by-layer assembly on organic electrochemical transistors," *ACS Appl. Mater. Interfaces*, vol. 9, no. 12, pp. 10427–10434, Mar. 2017, doi: 10.1021/acsami.6b15522.

[79] J. Peng *et al.*, "An organic electrochemical transistor for determination of microRNA21 using gold nanoparticles and a capture DNA probe," *Microchim. Acta*, vol. 185, no. 9, pp. 1–8, Sep. 2018, doi: 10.1007/s00604-018-2944-x.

[80] D. Khodagholy *et al.*, "*In vivo* recordings of brain activity using organic transistors," *Nature Commun.*, vol. 4, no. 1, p. 1575, Jun. 2013, doi: 10.1038/ncomms2573.

[81] J. Rivnay *et al.*, "High-performance transistors for bioelectronics through tuning of channel thickness," *Sci. Adv.*, vol. 1, no. 4, May 2015, Art. no. e1400251, doi: 10.1126/sciadv.1400251.

[82] A. Campana, T. Cramer, D. T. Simon, M. Berggren, and F. Biscarini, "Electrocardiographic recording with conformable organic electrochemical transistor fabricated on resorbable bioscaffold," *Adv. Mater.*, vol. 26, no. 23, pp. 3874–3878, Jun. 2014, doi: 10.1002/adma.201400263.

[83] X. Gu, C. Yao, Y. Liu, and I.-M. Hsing, "16-channel organic electrochemical transistor array for in vitro conduction mapping of cardiac action potential," *Adv. Healthcare Mater.*, vol. 5, no. 18, pp. 2345–2351, Sep. 2016, doi: 10.1002/adhm.201600189.

[84] F. Hempel *et al.*, "PEDOT:PSS organic electrochemical transistor arrays for extracellular electrophysiological sensing of cardiac cells," *Biosensors Bioelectron.*, vol. 93, pp. 132–138, Jul. 2017, doi: 10.1016/j.bios.2016.09.047.

[85] W. Lee *et al.*, "Nonthrombogenic, stretchable, active multielectrode array for electroanatomical mapping," *Sci. Adv.*, vol. 4, no. 10, Oct. 2018, Art. no. eaau2426, doi: 10.1126/sciadv.aau2426.

[86] G. Tarabella *et al.*, "A single cotton fiber organic electrochemical transistor for liquid electrolyte saline sensing," *J. Mater. Chem.*, vol. 22, no. 45, pp. 23830–23834, 2012, doi: 10.1039/c2jm34898e.

[87] J. D. Yuen, S. A. Walper, B. J. Melde, M. A. Daniele, and D. A. Stenger, "Electrolyte-sensing transistor decals enabled by ultrathin microbial nanocellulose," *Sci. Rep.*, vol. 7, no. 1, pp. 1–9, Feb. 2017, doi: 10.1038/srep40867.

[88] Y. Wang *et al.*, "Ion sensors based on novel fiber organic electrochemical transistors for lead ion detection," *Anal. Bioanal. Chem.*, vol. 408, no. 21, pp. 5779–5787, Aug. 2016, doi: 10.1007/s00216-016-9684-8.

[89] E. Bihar, Y. Deng, T. Miyake, M. Saadaoui, G. G. Malliaras, and M. Rolandi, "A disposable paper breathalyzer with an alcohol sensing organic electrochemical transistor," *Sci. Rep.*, vol. 6, no. 1, pp. 2–7, Sep. 2016, doi: 10.1038/srep27582.

[90] D. Khodagholy *et al.*, "Organic electrochemical transistor incorporating an ionogel as a solid state electrolyte for lactate sensing," *J. Mater. Chem.*, vol. 22, no. 10, pp. 4440–4443, 2012, doi: 10.1039/c2jm15716k.

[91] L. J. Currano, F. C. Sage, M. Hagedon, L. Hamilton, J. Patrone, and K. Gerasopoulos, "Wearable sensor system for detection of lactate in sweat," *Sci. Rep.*, vol. 8, no. 1, pp. 1–11, Dec. 2018, doi: 10.1038/s41598-018-33565-x.

[92] N. Coppedè, G. Tarabella, M. Villani, D. Calestani, S. Iannotta, and A. Zappettini, "Human stress monitoring through an organic cotton-fiber biosensor," *J. Mater. Chem. B*, vol. 2, no. 34, pp. 5620–5626, 2014, doi: 10.1039/c4tb00317a.

[93] X. Qing *et al.*, "Wearable fiber-based organic electrochemical transistors as a platform for highly sensitive dopamine monitoring," *ACS Appl. Mater. Interfaces*, vol. 11, no. 14, pp. 13105–13113, Apr. 2019, doi: 10.1021/acsami.9b00115.

[94] I. Gualandi, M. Marzocchi, A. Achilli, D. Cavedale, A. Bonfiglio, and B. Fraboni, "Textile organic electrochemical transistors as a platform for wearable biosensors," *Sci. Rep.*, vol. 6, no. 1, pp. 1–10, Sep. 2016, doi: 10.1038/srep33637.

[95] E. Battista *et al.*, "Enzymatic sensing with laccase-functionalized textile organic biosensors," *Organic Electron.*, vol. 40, pp. 51–57, Jan. 2017, doi: 10.1016/j.orgel.2016.10.037.

[96] Y. Wang *et al.*, "The woven fiber organic electrochemical transistors based on polypyrrole nanowires/reduced graphene oxide composites for glucose sensing," *Biosensors Bioelectron.*, vol. 95, pp. 138–145, Sep. 2017, doi: 10.1016/j.bios.2017.04.018.

[97] A. Yang *et al.*, "Fabric organic electrochemical transistors for biosensors," *Adv. Mater.*, vol. 30, no. 23, 2018, Art. no. 1800051, doi: 10.1002/adma.201800051.

[98] O. Parlak, S. T. Keene, A. Marais, V. F. Curto, and A. Salleo, "Molecularly selective nanoporous membrane-based wearable organic electrochemical device for noninvasive cortisol sensing," *Sci. Adv.*, vol. 4, no. 7, Jul. 2018, Art. no. eaar2904, doi: 10.1126/sciadv.aar2904.

[99] C. Yang, M. E. Denno, P. Pyakurel, and B. J. Venton, "Recent trends in carbon nanomaterial-based electrochemical sensors for biomolecules: A review," *Analytica Chim. Acta*, vol. 887, pp. 17–37, Aug. 2015, doi: 10.1016/j.aca.2015.05.049.

[100] A. P. Periasamy, Y. Umasankar, and S.-M. Chen, "Nanomaterials–Acetylcholinesterase enzyme matrices for organophosphorus pesticides electrochemical sensors: A review," *Sensors*, vol. 9, no. 6, pp. 4034–4055, May 2009, doi: 10.3390/s90604034.

[101] F. Ricci, G. Volpe, L. Micheli, and G. Palleschi, "A review on novel developments and applications of immunosensors in food analysis," *Analytica Chim. Acta*, vol. 605, no. 2, pp. 111–129, Dec. 2007, doi: 10.1016/j.aca.2007.10.046.

[102] F. Ricci, G. Adornetto, and G. Palleschi, "A review of experimental aspects of electrochemical immunosensors," *Electrochim. Acta*, vol. 84, pp. 74–83, Dec. 2012, doi: 10.1016/j.electacta.2012.06.033.

[103] A. J. Bandodkar and J. Wang, "Non-invasive wearable electrochemical sensors: A review," *Trends Biotechnol.*, vol. 32, no. 7, pp. 363–371, Jul. 2014, doi: 10.1016/j.tibtech.2014.04.005.

[104] D. A. Bernards, D. J. Macaya, M. Nikolou, J. A. DeFranco, S. Takamatsu, and G. G. Malliaras, "Enzymatic sensing with organic electrochemical transistors," *J. Mater. Chem.*, vol. 18, no. 1, pp. 116–120, 2008, doi: 10.1039/b713122d.

[105] E. Kim *et al.*, "A glucose sensor based on an organic electrochemical transistor structure using a vapor polymerized poly (3, 4-ethylenedioxythiophene) layer," *Jpn. J. Appl. Phys.*, vol. 49, no. 1, 2010, Art. no. 01AE10, doi: 10.1143/jjap.49.01ae10.

[106] I. Gualandi, D. Tonelli, F. Mariani, E. Scavetta, M. Marzocchi, and B. Fraboni, "Selective detection of dopamine with an all PEDOT:PSS organic electrochemical transistor," *Sci. Rep.*, vol. 6, no. 1, pp. 1–10, Dec. 2016, doi: 10.1038/srep35419.

[107] N. Wang, Y. Liu, Y. Fu, and F. Yan, "AC measurements using organic electrochemical transistors for accurate sensing," *ACS Appl. Mater. Interfaces*, vol. 10, no. 31, pp. 25834–25840, Aug. 2018, doi: 10.1021/acsami.7b07668.

[108] J.-A. Chou *et al.*, "Organic electrochemical Transistors/SERS-active hybrid biosensors featuring gold nanoparticles immobilized on thiol-functionalized PEDOT films," *Frontiers Chem.*, vol. 7, pp. 1–12, Apr. 2019, doi: 10.3389/fchem.2019.00281.

[109] B. Crone *et al.*, "Large-scale complementary integrated circuits based on organic transistors," *Nature*, vol. 403, no. 6769, pp. 521–523, Feb. 2000, doi: 10.1038/35000530.

[110] D. Nilsson, T. Kugler, P. O. Svensson, and M. Berggren, "An all-organic sensor-transistor based on a novel electrochemical transducer concept printed electrochemical sensors on paper," *Sens. Actuators B, Chem.*, vol. 86, nos. 2–3, pp. 193–197, 2002, doi: 10.1016/S0925-4005(02)00170-3.

[111] D. Nilsson, M. Chen, P. Svensson, N. D. Robinson, T. Kugler, and M. Berggren, "All-organic electrochemical device with bistable and dynamic functionality," *Proc. SPIE*, vol. 5051, pp. 468–476, Jul. 2003.

[112] G. Maltezos, R. Nortrup, S. Jeon, J. Zaumseil, and J. A. Rogers, "Tunable organic transistors that use microfluidic source and drain electrodes," *Appl. Phys. Lett.*, vol. 83, no. 10, pp. 2067–2069, Sep. 2003, doi: 10.1063/1.1609056.

[113] M. Taniguchi and T. Kawai, "Vertical electrochemical transistor based on poly(3-hexylthiophene) and cyanoethylpullulan," *Appl. Phys. Lett.*, vol. 85, no. 15, pp. 3298–3300, Oct. 2004, doi: 10.1063/1.1801167.

[114] J. T. Mabeck, J. A. DeFranco, D. A. Bernards, G. G. Malliaras, S. Hocdé, and C. J. Chase, "Microfluidic gating of an organic electrochemical transistor," *Appl. Phys. Lett.*, vol. 87, no. 1, Jul. 2005, Art. no. 013503, doi: 10.1063/1.1991979.

[115] D. Nilsson, "An organic electrochemical transistor for printed sensors and logic," Ph.D. dissertation, Dept. Sci. Technol., Linkoping Stud. Sci. Technol., Linkopings Univ., Norrkoping, Sweden. [Online]. Available: https://www.diva-portal.org/smash/get/diva2:20961/FULLTEXT01.pdf

Marios Sophocleous (Member, IEEE) received the M.Eng. degree in mechatronics and the Ph.D. degree in thick-film underground sensors from the University of Southampton in 2016. He has been a Special Scientist with the University of Cyprus since 2016. He is an active member of the IEEE community, whilst he has also been invited multiple times as a technical and/or organizing committee member for major conferences.

Laura Contat-Rodrigo received the M.Sc. and Ph.D. degrees from the Universitat de València, Spain, in 1995 and 2000, respectively. She is an Assistant Professor with the Universitat Politècnica de València, and a member of the Institute of Molecular Recognition and Technological Development (IDM), Spain. Her research interest includes the development of chemical sensors based on organic thin film transistors.

Eduardo García-Breijo received the M.S. degree in electronic engineering from the Universitat de València (UV), Spain, in 1997, and the Ph.D. degree from the Universidad Politécnica de Valencia (UPV), in 2004. He is an Assistant Professor of Electronic Technologies with UPV, where he is a member of the Instituto de Reconocimiento Molecular y Desarrollo Tecnológico. His main research interest includes the development of printed sensors.

Julius Georgiou (Senior Member, IEEE) received the M.Eng. degree in electrical and electronic engineering and the Ph.D. degree from Imperial College London, London, U.K., in 1998 and 2003, respectively. He is an Associate Professor with the University of Cyprus. His research interests include low-power analog and digital ASICs, implantable biomedical devices, bioinspired electronic systems, brain–computer-interfaces (BCIs), and semiconductor device design. He is a member of the IEEE Circuits and Systems Society, the BioCAS Technical Committee, and the IEEE Circuits and Systems Society Analog Signal Processing Technical Committee.